Scanning Microscopy Vol. 12, No. 4, 1998 (Pages 553-583) 0891-7035/98$5.00+.25
Scanning Microscopy International, Chicago (AMF O'Hare), IL 60666 USA

# SURFACE ANALYTICAL STUDIES OF OXIDATION AND COLLECTOR ADSORPTION IN SULFIDE MINERAL FLOTATION

Roger St.C. Smart*, John Amarantidis, William Skinner, Clive A. Prestidge, Lori LaVanier[1] and Stephen Grano

Ian Wark Research Institute, University of South Australia, The Levels, South Australia 5095
[1]Physical Electronics, 6059 Flying Cloud Drive, Eden Prairie, Minnesota 55344

(Received for publication May 7, 1995 and in revised form March 7, 1996)

## Abstract

The physical and chemical forms of sulfide mineral surfaces are reviewed. The initial surfaces and oxidation products have been studied by scanning Auger microscopy, X-ray photoelectron spectroscopy, scanning tunneling microscopy, atomic force microscopy, scanning electron microscopy and time-of-flight secondary ion mass spectrometry. Changes to surface speciation as a function of time, pH, Eh and collector adsorption, related to mineral flotation, have been followed with these techniques. Oxidation products are formed in different processes, namely: metal-deficient sulfides, polysulfides and sulfur; oxidized fine sulfide particles; colloidal hydroxide (e.g., $Fe(OH)_3$, $Pb(OH)_2$) particles and flocs; continuous surface layers (e.g., hydroxide, oxyhydroxide, oxide species) of varying depth; sulfate and carbonate species; isolated, patchwise and face-specific oxide, hydroxide and hydroxycarbonate development. The actions of collector molecules (e.g., xanthate, dithiophosphinates) have been identified in various modes, namely: adsorption to specific surface sites; colloidal precipitation from solution; detachment of small sulfide particles from larger particle surfaces; detachment of small oxide/hydroxide particles; removal of adsorbed and amorphous oxidized surface layers; inhibition of oxidation; disaggregation of larger particles; and patchwise or face-specific coverage. The different modes of oxidation and collector action are exemplified using case studies from the literature and recent research.

**Key Words**: Sulfides, surface oxidation, flotation, adsorption.

*address for correspondence:
Roger St.C. Smart, address as above.
Telephone number: (08) 302-3353
FAX number: (08) 302-3683
E.mail: roger.smart@levels.unisa.edu.au

## Introduction

The process of selective separation of valuable sulfide minerals from gangue (e.g., other non-valuable sulfide minerals, oxides, silicates, etc.) is heavily dependent on processing steps involving control of surface oxidation products on the mineral surfaces and the addition of collector molecules designed to induce a hydrophobic surface for bubble-particle attachment. Separation is then achieved by flotation of the valuable mineral into the froth collected from the top of the flotation cell. The complex nature of this process is well established both from plant operation and laboratory research (Smart, 1991; Richardson, 1995; Shannon and Trahar, 1996). To describe the full set of complexities would fill, and indeed has filled, several books (Fuerstenau, 1976; Leja, 1982; Forssberg, 1986; Somasundaran, 1986; Laskowski and Ralston, 1992). In this review, we will focus on the use of scanning and imaging surface analytical techniques applied to the study of sulfide surfaces in flotation. In this context, it is useful to identify some of these complexities that will be relevant to later discussion. They include:

(**1**) chemical alteration of the surface layers of the sulfide minerals induced by oxidation reactions in the pulp solution;

(**2**) the presence of a wide range of particle sizes in the ground sulfide ores;

(**3**) galvanic interactions between different sulfide minerals to produce different reaction products on the mineral surfaces;

(**4**) interaction between particles in the form of aggregates and flocs;

(**5**) the presence of colloidal precipitates arising from dissolution of the sulfide minerals and grinding media;

(**6**) the mechanism of adsorption of reagents to specific surface sites;

(**7**) competitive adsorption between oxidation products, conditioning reagents and collector reagents.

The chemically altered layers on the surfaces of metal sulfides, particularly as oxides and hydroxides, are known to interfere with the recovery and selectivity of minerals separation by flotation (Guy and Trahar, 1985;

Zachwieja *et al*., 1989; Grano *et al*., 1990; Kristall *et al*., 1994; Grano *et al*., 1995). As part of the complete description of flotation chemistry, it is clearly necessary to understand the chemical and physical forms of these layers and the changes that occur in them during conditioning and flotation. The range of information available from the effective use of surface sensitive techniques has greatly assisted this understanding. The techniques have included scanning Auger microscopy (SAM), X-ray photoelectron spectroscopy (XPS), scanning tunneling microscopy (STM), atomic force microscopy (AFM), analytical scanning electron microscopy (SEM) and the recent application of time-of-flight secondary ion mass spectrometry (TOF-SIMS). We will concentrate on two specific aspects of the surface layers, namely surface oxidation and the effects of collector addition on these layers, with applications drawn from both research on single minerals/mineral mixtures and plant practice.

## Techniques

Several surface sensitive techniques, capable of analyzing the first few atomic layers of the mineral surface, have been used for more than ten years in a variety of studies related to the mechanisms of oxidation and adsorption in sulfide mineral flotation. The significance of these techniques is that they provide not only a compositional analysis of the surface but also information on chemical states (e.g., oxidation, bonding) and spatial distribution of adsorbed species on individual particles and complex mixtures of minerals as a function of depth through the surface layers. It is recognized that, since they are *ex situ* techniques that operate in ultra high vacuum, validation of the relationship between the measured surface compositions or chemical states and those prevailing in the original pulp solution in the flotation cell or circuit, is required. Sampling methodologies have been developed and tested over extensive (i.e., more than 500 samples) sets of correlated surface analysis/flotation response testing in major projects in Australia (AMIRA, 1992, 1994) and Canada (Stowe *et al*., 1995). Surface chemical changes corresponding to changes in process conditions have been clearly demonstrated in this work. In one sampling methodology (Smart, 1991), the sample is taken directly from the circuit or cell, dissolved oxygen is removed from the solution before freezing, and the thawed slurry is introduced to the spectrometer without air exposure of the mineral surfaces. The majority of the solution phase is removed (or exchanged) by decantation before evaporation in the fore-vacuum of the spectrometer. In a second approach (Chryssoulis, 1994), the sample is size-separated, washed and dried under vacuum before being stored under an inert gas or vacuum. The storage vials contain silica-gel to remove residual moisture and are transported in frozen condition.

Single mineral studies of surface oxidation and adsorption of collector molecules have used a variety of sample preparation procedures for the mineral surfaces. These have included fracture under high vacuum, surface abrasion under inert gas followed by transfer to the spectrometer, washing by water or prepared pH/Eh solutions, and solid powders pressed into conductive tape or soft metal substrates.

The characteristics and operating conditions of SAM, XPS, SEM and TOF-SIMS techniques have been fully described in previous publications (Smart, 1991; O'Connor *et al*., 1992; Chryssoulis, 1994). STM and AFM studies of mineral surfaces and their oxidation have also been described in a review (Hochella, 1995) and several papers (Laajalehto *et al*., 1993; Kim *et al*., 1995). These techniques have provided important complementary information to that from SAM and SEM, with resolution down to atomic scale.

## Surface Oxidation

It is well established that all metal sulfide minerals exhibit oxide and hydroxide species on their surface after exposure to air or aqueous solution. They have been observed in studies of pyrite (Buckley *et al*., 1985; Buckley and Woods, 1987), pyrrhotite (Buckley and Woods 1985a,b; Jones *et al*., 1992; Pratt *et al*., 1994), chalcopyrite (Buckley and Woods, 1984a; Zachwieja *et al*., 1989; Smart, 1991), galena (Buckley and Woods, 1984b; Fornasiero *et al*., 1994), pentlandite (Richardson and Vaughan, 1989; Buckley and Woods, 1991a), cobaltite (Buckley, 1987) and sphalerite (Buckley *et al*., 1989a,b,c; Prestidge *et al*., 1994). However, the mechanisms of surface oxidation are substantially different between different sulfides and are influenced by variables such as conditioning time, pH, Eh and the gas atmosphere above the sample.

Evidence from the combination of techniques has now shown that the mechanisms of oxidation are considerably more complex than those represented by simple reactions such as:

$$MS + xH_2O + 1/2xO_2 \rightarrow M_{1-x}S + xM(OH)_2 \qquad (1)$$

where MS represents a metal sulfide.

The chemical nature of the $M_{1-x}S$ product, the spatial distribution of the oxidation products, dissolved and reprecipitated species, other higher oxidation products (e.g., sulfate) and interactions with other dissolved species (e.g., $CO_2$) all complicate the real situation. As examples from the case studies below will show, hydroxide products are not formed uniformly over the surface of the sulfide mineral, the chemical form of the metal deficient or sulfur-rich surface is

highly variable, and the presence of small, oxidized particles and particle interactions must be considered.

The mechanisms of surface oxidation and the consequent physical and chemical forms of oxidation products on the surface, derived from studies using the surface analytical techniques, can be summarized as:

(**1**) metal deficient (sulfur-rich), oxide surfaces, polysulfides and elemental sulfur;

(**2**) oxidized fine particles attached to larger sulfide particle surfaces;

(**3**) colloidal metal hydroxide particles and flocs;

(**4**) continuous surface layers (e.g., oxide/hydroxide) of varying depth;

(**5**) formation of sulfate and carbonate species;

(**6**) non-uniform spatial distribution with different oxidation rates, e.g., isolated, patchwise oxidation sites, face specificity.

Each of these oxidation mechanisms will now be discussed using evidence from published literature and research undertaken in our own group. In reviewing the research literature, it rapidly becomes apparent that a myriad of different oxidation and adsorption conditions have been used. Comparisons are complicated by differences in oxidising atmospheres (e.g. air, $O_2$), solution conditions (e.g. pH, Eh), added species (e.g. dissolved, colloidal), temperatures and times. Similarly, for collector adsorption studies, different preconditioning (e.g., oxidation), molecular structures, concentrations and conditioning times are found in most papers. We have attempted to place the studies in some systematic order and to distinguish different regimes based on particular factors where possible. The remaining research issues, identified at the end of this review, note that the dependence of surface chemistry and flotation on a number of these factors is still distinctly unclear.

Where studies are available, we have ordered results on different minerals in the sequence: pyrite, pyrrhotite, chalcopyrite, pentlandite, galena, sphalerite, and other sulphide minerals.

## Case Studies of Oxidation Mechanisms

### Metal deficient sulfides, polysulfides and elemental sulfur

It is now well established that iron-containing sulfide minerals (e.g., pyrite, pyrrhotite, chalcopyrite, pentlandite) essentially follow a reaction mechanism similar to that in Equation 1 in that iron hydroxide products and an underlying metal-deficient or sulfur-rich sulfide surface are formed. The seminal work of Buckley, Woods and their colleagues, using a combination of XPS and electrochemical techniques, has clearly demonstrated this mechanism in single mineral studies. The oxidation of abraded pyrite surfaces exposed to air for a few minutes produces a high binding energy doublet component of the S2p spectrum in addition to ferric oxide/hydroxide reaction products (Buckley and Woods, 1987). The sulfur product can now be attributed to an iron-deficient $Fe_{1-x}S_2$ surface layer in which polysulfide-like species $S_n^{2-}$ are formed. Specifically, Mycroft *et al*. (1990) have correlated XPS and Raman spectra of electrochemically oxidized pyrite surfaces with polysulfide model compounds. Collectorless flotation of pyrite in alkaline solution, correlated to electrochemical oxidation, can be explained by the production of a hydrophobic sulfur-rich surface together with hydrophilic iron hydroxide species (Ahlberg *et al*., 1990). After grinding, the surface becomes substantially covered by the hydrophilic species, and no significant flotation is observed without addition of collector. Collectorless flotation can, however, be easily obtained after complexing the iron with ethylenediaminetetraacetic acid (EDTA) in solution, indicating that the underlying hydrophobic sulfur-rich layer is responsible for pyrite flotation under these conditions. It is noted that elemental sulfur was not evident at pyrite surfaces exposed to air or neutral to alkaline solutions (Buckley *et al*., 1985; Buckley and Woods, 1987). Thin layers of elemental sulfur were, however, observed on pyrite surfaces exposed to aerated, dilute sodium sulfide solutions (Buckley and Woods, 1987; McCarron *et al*., 1990). Prolonged exposure of the pyrite to solution resulted in the appearance of sulfate, together with the ferric oxide/hydroxide, in the surface layers (see below).

Similarly, pyrrhotite surfaces oxidized in air or aqueous solution form iron oxide/hydroxide and iron-deficient sulfide surfaces (Buckley and Woods, 1985a,b). In mildly acidic solution, a soluble iron product is formed, leaving a surface sulfur species with a S2p binding energy only 0.2 eV less than that for elemental sulfur. In contrast, alkaline solutions resulted in ferric hydroxide, sulfate species and iron-deficient sulfide. As with pyrite, electrochemical oxidation to Eh > 400 mV produced both elemental sulfur and sulfate species.

Further evidence for the mechanism of formation of the sulfur-rich surface has come from combined XPS and X-ray difffraction (XRD) studies of pyrrhotite surfaces exposed to air, water and deoxygenated acid solution (Jones *et al*., 1992). After acid reaction, the surface partly restructures to a crystalline, defective tetragonal $Fe_2S_3$ product in which linear chains of $S_n$ atoms have a S-S distance similar to elemental sulfur but the high binding energy doublet S2p associated with the sulfur-rich surface is still 0.2 eV less than that of $S_8$. The shift to high binding energy proceeds systematically from 1.0 to 1.8 eV as the reaction progresses. Combined XPS and SAM studies of air-oxidized pyrrhotite surfaces (Pratt *et al*., 1994; Mycroft *et al*., 1995) add further evidence to the oxidation mechanism with the observation of monosulfide through disulfide to polysulfide species. After 50 hours of air oxidation, three compositional zones are found with the outermost iron and oxygen-rich layer < 1 nm thick and a sulfur-rich layer beneath

displaying a continuous, gradual decrease in S/Fe ratio through to the unaltered pyrrhotite. These studies have also demonstrated the presence of ~30% Fe(III) in the natural pyrrhotite surface freshly fractured under high vacuum.

Chalcopyrite also oxidizes with the formation of a ferric oxide/hydroxide overlayer and an iron-deficient sulfur-rich, copper-rich underlying sulfide in air or alkaline solution (Buckley and Woods, 1984a; Luttrell and Yoon, 1984). It is not yet clear whether a specific copper sulfide phase is formed in the reacted sulfide surface: CuS (Luttrell and Yoon, 1984), and $CuS_2$ (Buckley and Woods, 1984) have both been suggested. The collectorless flotation of chalcopyrite after air exposure or solution oxidation has been directly correlated with the surface composition determined by XPS (Zachweija *et al*., 1989). Removal of iron hydroxide species during conditioning in alkaline solution, to leave the hydrophobic sulfur-rich sulfide surface, showed strong flotation. Conversely, oxidized chalcopyrite surfaces reduced *in situ* become copper deficient and were not able to float.

The iron-containing pentlandite $(Fe, Ni)_9S_8$ mineral has also been studied with similar results using XPS, SAM, Mössbauer and spectral reflectance measurements. Oxidation of the pentlandite surfaces gives ~1 nm thickness layer of iron oxide/hydroxide, with later appearance of nickel oxides/hydroxides and sulfate species, and the formation of a sulfur-rich, nickel-rich subsurface layer (Richardson and Vaughan, 1989; Buckley and Woods, 1991a). In dilute acid, the oxide/hydroxide layer is largely soluble, whereas in alkaline media, the products were similar to those from air oxidation but the reaction rate was faster. The resulting sub-surface is believed to restructure from pentlandite to violarite $FeNi_2S_4$ (Richardson and Vaughan, 1989).

Galena surface oxidation proceeds by considerably different and more complex mechanisms. In air, initial stages of the oxidation show (XPS and STM) the PbS surface becoming enriched in lead oxide/hydroxide and carbonate species (Buckley and Woods, 1984b; Laajalehto *et al*., 1993). The spatial distribution of those products is described later. However, no metal-deficient sulfide S2p high binding energy shift is observed and sulfate species are only observed after extended exposure to air.

It appears that metal-deficient sulfide species lie under the isolated hydroxide and carbonate patches. Their contribution to the S2p signal is depth-attenuated and, with the low surface coverage by the oxidation products, they do not make a significant contribution to the S2p components. More recently, Kartio *et al*. (1994) have demonstrated, using synchrotron radiation tuned close to the XPS signal, that the information obtained may be limited by surface sensitivity. Optimal XPS surface sensitivity is only attained with kinetic energies of the exciting XPS electrons in the region 30-100 eV where the escape depth is typically a fraction of a nanometer. For pyrite (100) surfaces cleaved in ultra high vacuum, two new types of sites corresponding to surface states of $FeS_2$ and FeS type in addition to bulk $FeS_2$ states, were found (Karthe *et al*., 1993). In contrast, the (100) surface of a cleaved galena crystal does not give any evidence for additional states in the Pb4f or S2p spectra (Kartio *et al*., 1994). Synchrotron studies of S2p states at different depths on galena surfaces oxidized in air may help to resolve the form of the oxidized sulfur.

In neutral or alkaline aqueous solution, oxidation proceeds on galena surfaces without the formation of metal-deficient sulfur-rich, polysulfide or elemental sulfur zones as seen in combined XPS, dissolution kinetics and STM studies (Laajalehto *et al*., 1993; Fornasiero *et al*., 1994; Kim *et al*., 1994, 1995). The mechanism of oxidation apparently involves the congruent dissolution of lead and sulfide ions, their oxidation/hydrolysis in solution or near the surface with the formation of lead oxide/hydroxide, lead hydroxy carbonate and sulfur oxy species (e.g., $S_2O_3^{2-}$, $SO_4^{2-}$). Dissolution occurs from spatially separated pits on the surface, but XPS also finds lead hydroxy and carbonate surface species. The dissolution products may be subsequently readsorbed or precipitated on the galena surface at higher solution concentration.

Under acidic conditions, metal-deficient sulfide or polysulfide phases have been detected by both XPS (Buckley and Woods, 1984b) and SAM (P. Bandini, C.A. Prestidge, J. Ralston and R.St.C. Smart, unpublished results). The oxidation mechanism is apparently incongruent:

$$n(PbS) \rightarrow Pb_{n-x}S_n + xPb^{2+} + 2xe^- \qquad (2)$$

with the metastable, sulfur-rich surface presumably responsible for the strong collectorless flotation under acidic conditions.

Hydrodynamic conditions can also extensively influence the form of the galena mineral surfaces. Shear conditions and dilution during cyclosizing have been shown (Prestidge and Ralston, 1995a) to enhance the incongruent dissolution of galena, removing the lead hydroxide species and exposing metal-deficient sulfide or polysulfide surfaces with high measured contact angles and flotabilities.

There has been some controversy surrounding the nature of the surface species formed during mineral oxidation and, in particular, which species (i.e., metal-deficient sulfides, polysulfides or elemental sulfur) are responsible for the collectorless flotation of galena (Buckley, 1994). Evidence has been provided that elemental sulfur can be extracted with cyclohexane from floated wet-ground pyrrhotite (Heyes and Trahar, 1984) and recently multilayer quantities of sulfur were apparently extracted from dry-ground galena and chalcopyrite (Kelebek and Smith, 1989). Buckley and Riley (1991) have, however, shown that whilst

**Figure 1**. Field emission scanning electron micrograph of a ground chalcopyrite surface conditioned in water for 1.5 hours. then reground immediately before imaging. The fresh fracture face on the left hand side can be contrasted with the oxidized face on the right.

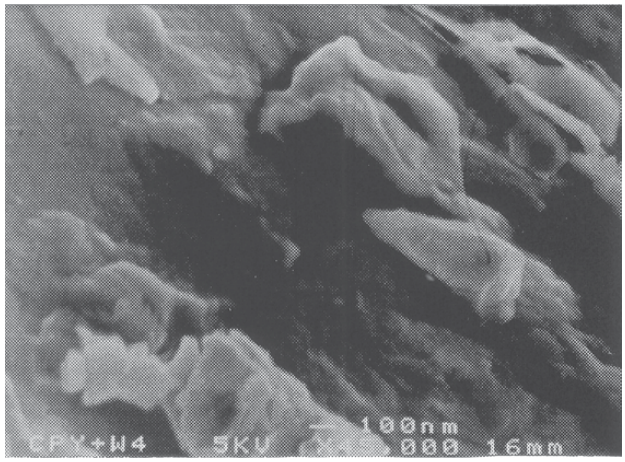


**Figure 2**. Oxidized surface of sample as in Figure 1 at higher magnification.

ethanol does extract a sulfur species from galena, sulfur is not present in elemental form on the freshly ground mineral surface, as evidenced by sequentially cooled samples in XPS spectra. Cyclohexane did not extract the same sulfur species. It remains possible that the elemental sulfur extracted by ethanol may have been transformed from polysulfide species on the mineral surface during extraction or that the solvent may have chemically altered the surface. It is also not simple to distinguish elemental $S_8$ from polysulfide species in UV-visible spectra.

Other aspects of this controversy with relevant references are summarized in the discussion from the Workshop on Flotation-Related Surface Chemistry of Sulfide Minerals (Walker *et al*., 1989).

The surface oxidation of sphalerite has been less systematically studied than those of other sulfide minerals but the pattern of reaction appears to be similar. After 3 weeks in air or conditioning in alkaline solution (1 hour), there are no significant changes in the Zn Auger peak ($L_3M_{4,5}M_{4,5}$) or S2p peaks and very little evidence for oxidized products. It has been suggested that sphalerite oxidizes considerably more slowly than the other sulfide minerals under these conditions (Buckley *et al*., 1989a). Further study of ZnS oxidation using STM/AFM with XPS is still required.

In contrast, under acid leaching conditions, dissolution of zinc occurs with the formation of a metal-deficient sulfide layer. Under oxidative leaching conditions, the metal-deficient sulfide is again observed in thicker layers and, at high acid concentrations, elemental sulfur (~10%) was also formed protecting the sphalerite from further leaching (Buckley *et al*., 1989c). With addition of 0.1 M Fe(III) under these conditions, thick layers of elemental sulfur developed.

In general, given the different rates of reaction and congruency/incongruency differences in dissolution between the different sulfides, the mechanisms of formation of metal-deficient sulfide are quite similar. In neutral or alkaline solution, oxide/hydroxide and hydroxy carbonate species are formed. Fe(III) oxidized species remain on the surface; Pb(II) and Zn(II) species initially dissolve and then reprecipitate. The underlying mineral is left metal-deficient producing, for iron-containing sulfides polysulfide $S_n^{2-}$ species but, for PbS, soluble sulfur-oxy species. After prolonged periods in solution, all surfaces show the formation of sulfate ions. In acid conditions, the removal of the metal oxide/hydroxide species (at different pH for each metal), exposes a metal-deficient sulfide surface with hydrophobic character for all of the sulfides studied to date. Elemental sulfur is only found after severe acid leaching, in highly oxidative (Eh > 400 mV) solutions, or after the addition of sodium sulfide in conditioning. The evidence that the metal-deficient sulfide surface corresponds to polysulfide species is now quite strong (Mycroft *et al*., 1990; Jones *et al*., 1992). At least some forms of these polysulfides can clearly impart hydrophobicity (Prestidge and Ralston, 1995a) and mineral flotability.

**Oxidized fine sulfide particles**

The presence of oxidized fine particles (< 2 μm) attached to larger sulfide mineral surfaces has been established in the SAM/XPS work of Smart (1991). The removal of fine particles by successive ultrasonication/ decantation, from ground pyrite surfaces was shown to

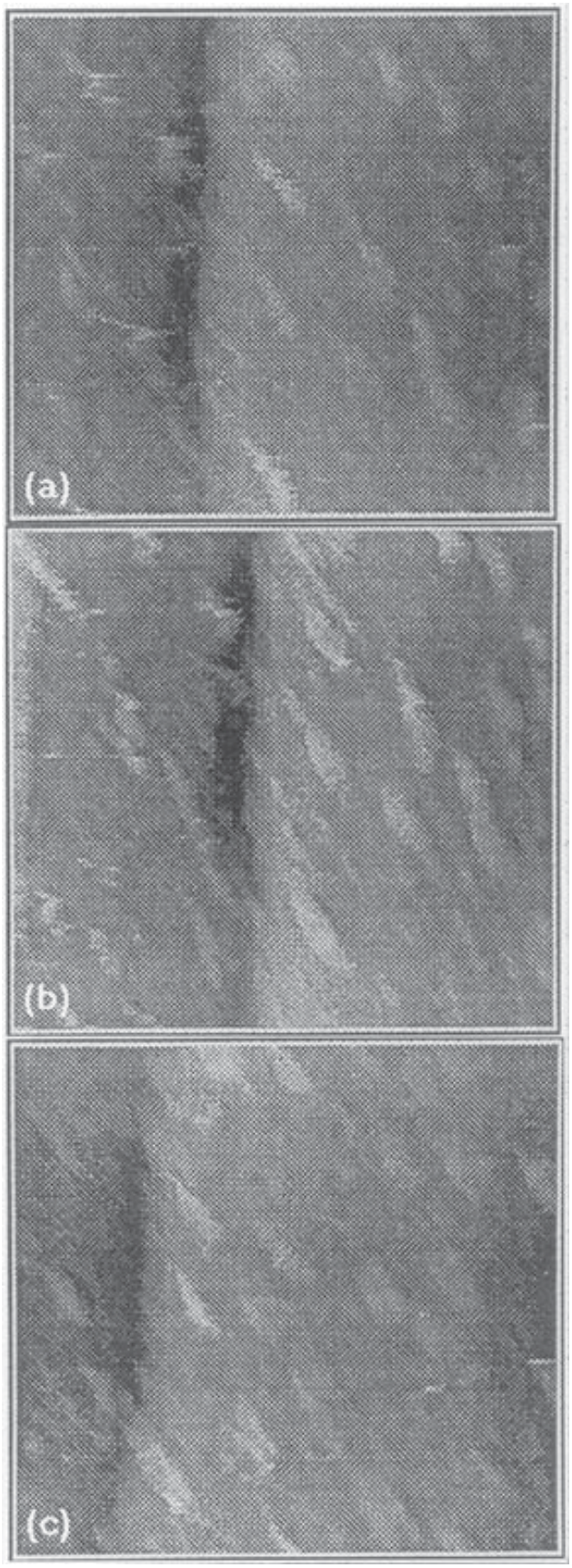


**Figure 3**. Top-view STM images of galena treated with $10^{-3}$ M lead (II) ions at pH 7, as a function of time (xy scale = 500 nm): (**a**) 10 minutes (z scale = 11.2 nm), (**b**) 30 minutes (z scale = 13.7 nm) and (**c**) 50 minutes (z scale = 15.4 nm). Constant current mode (0.2-0.25 nA), bias ~0.35 V.

systematically reduce the surface oxygen concentration (as hydroxide O1s at 531.5 eV binding energy) for pyrite from ~40 at.% to ~22 at.%. Ion etching this surface to 25 nm depth without removal of the attached fine particles reduced the oxygen concentration to ~28% but, after fine particle removal, ion etching effectively removed all of the hydroxide from the surface. Chalcopyrite surfaces behaved similarly but were less oxidized.

The physical nature of the oxidized layer formed initially on these surfaces can be seen in Figure 1 where a chalcopyrite sample, ground initially in distilled water and allowed to condition for 1.5 hours, was reground at that time and examined immediately using high resolution field emission SEM without coating at 5 kV.

The oxidized surface layer and fine oxidized particles are clearly visible on the conditioned surface at the lower right of the micrograph with the fracture face, and newly fractured fine particles on this fresh face, at upper left of the micrograph.

The surface layer, at high magnification in other micrographs, appears to be relatively thin, i.e., of the order of 10 nm (Fig. 2). The secondary electron image clearly illustrates a chemical and physical difference between the oxidized, conditioned surface and the fractured face exposed to the solution for only a few minutes. Similar images are obtained from fractured pyrite surfaces prepared using the same methodology. In general, SEM and SAM images from pyrite and chalcopyrite surfaces examined in the early stages of oxidation show two general features, namely oxidized fine particles apparently attached to larger particle surfaces and continuous oxidized layers formed on both large and fine particle surfaces. At higher magnification, as in Figure 2, it is apparent that fine particles expose a wide variety of different facets, morphologies and sizes (from dimensions less than 50 nm to several micrometers).

The attached oxidized fine sulfide particles are not easily removed by sedimentation/decantation techniques (Smart, 1991). Successive ultrasonication/ decantation (8 cycles) reduces the surface concentration of attached fine particles but the shearing action of the cyclosizer produces larger particles almost completely free of adhering fine particles (Greet and Smart, 1996). Additionally, cyclosizing resulted in considerably reduced surface oxygen concentrations, greater exposure of sulfide minerals and

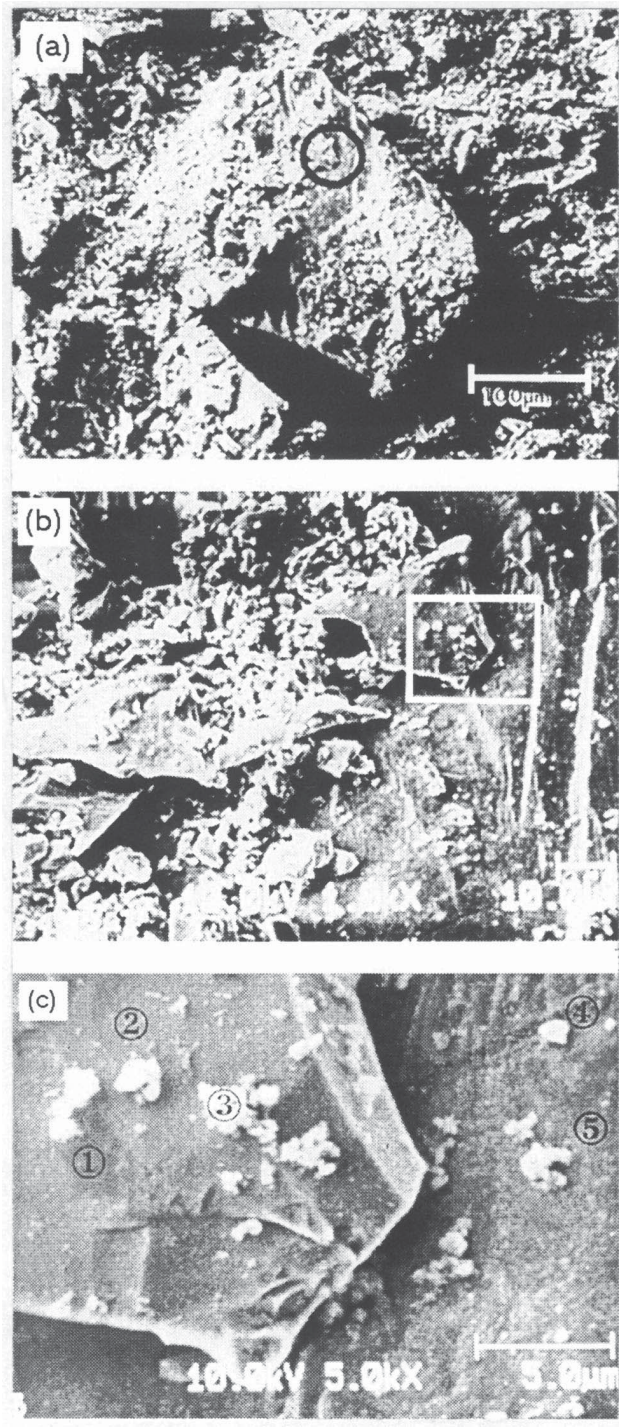


**Figure 4**. SAM images from particles at successively higher magnification, i.e., white bar = (**a**) 100 μm, (**b**) 10 μm and (**c**) 5 μm. Note the five marked points (i.e., 1-5) for Auger analysis in Figure 4c. (Smart, 1991). Oxygen depth profiles gave approximately 5, 30, > 300, 80, 10 nm, respectively for each point.

thinner layers of oxidation products. The oxidized fine particles are clearly strongly adsorbed to the oxidized surfaces of larger particles. These hydrophilic fine particles may, on the one hand, reduce the hydrophobicity of larger particles and flotation selectivity. On the other hand, the attached particles may also be collected to the concentrate, thereby affecting flotation grade. Size-by-size assays are affected by the removal of these fine particles from coarser particle surfaces during cyclosizing, particularly in assays of the finest fractions (Greet and Smart, 1996).

**Colloidal metal hydroxide particles and flocs**

The SAM results reported by Smart (1991) have shown that $Fe(OH)_3$ flocs form on the surface of pyrite and chalcopyrite particles conditioned for relatively long periods (> 14 days) in nitrogen-purged pH 9 solution. These flocs comprise clumps of loose aggregates, with dimensions 1-3 μm, consisting of smaller spheroidal particles each with approximate diameters of 0.1-0.5 μm. They are not observed on similar surfaces conditioned for shorter periods (i.e., several hours) but have been seen in plant samples following fine grinding in which accelerated dissolution of pyrrhotite and iron grinding media has occurred (AMIRA, 1992, 1994). They appear to have been precipitated from saturated ferric hydroxide solution as colloidal $Fe(OH)_3$ particles. Mechanical agitation or ultrasonication/decantation easily removes these flocs from the sulfide surfaces, showing that they are only weakly bonded to the oxidized sulfide minerals.

Colloidal iron oxide particles prepared synthetically in solution as small spheroids can be attached to galena surfaces, following classical particle adsorption isotherms, to full monolayer coverage at pH values below 6 (P. Bandini, C.A. Prestidge, J. Ralston and R.St.C. Smart, unpublished results). In the pH range of 6 to 10, electrostatic repulsion between iron oxide particles and unoxidized galena surfaces opposes adsorption. Adsorption in this pH range is due to attractive interactions or hydrogen bonding between iron oxide and oxidized regions on the galena surface. The mechanism for the interaction of hydrolysed iron (III) species with galena surfaces also appears to rely largely on electrostatic interactions (Prestidge *et al*., 1995). The highest adsorption densities occur at pH 2-4 and pH 10-11 with values significantly higher than those in the intermediate pH range. Iron (III) adsorption densities, determined from EDTA extraction, have been shown to give excellent agreement with surface atomic concentrations determined from XPS analysis. The adsorption is dramatically influenced by iron (III) concentration, pH and the extent of galena oxidation. At pH values between 2 and 4, the galena surface is weakly negatively charged, whereas the iron hydroxide species, e.g., $Fe(OH)_2^+$, are positively charged. Under alkaline conditions, oxidized galena surfaces with lead hydroxy groups (isoelectric point, iep, near pH 10) may interact with negatively charged iron species, e.g., $Fe(OH)_4^-$.

*In situ* STM images of galena surfaces in the presence of $10^{-3}$ M $Pb^{2+}$ ions at pH 7 have also shown the development of elongated, oval colloidal projections with dimensions of ~50 nm x 20 nm (Kim *et al*., 1995). The spatial distribution on the surface displays a directionality apparently corresponding to the [110] lattice directions of the galena surface (Fig. 3). XPS analysis has confirmed that these species are predominantly lead hydroxide, presumably formed from the hydrolysis of lead ions followed by surface attachment. It is not yet clear whether the mechanism of surface attachment involves the formation of lead hydroxide colloids in solution and their precipitation on to the galena surface or adsorption of $Pb^{2+}/Pb(OH)_2$ molecular species at specific sites on the galena surface before *in situ* growth. However, the formation of these patchy surface layers shows that the galena surface is heterogeneous and that its overall hydrophobicity and flotation response will be controlled not only by the surface chemistry but by the surface arrangement of hydrophilic and hydrophobic patches (see below).

**Continuous oxide/hydroxide surface layers**

The presence of continuous layers of metal hydroxide products, particularly iron hydroxides, can be directly inferred from the case studies in the previous sections where longer periods of conditioning in air-saturated solutions, electrochemical oxidation and *in situ* dissolution/precipitation has occurred. SAM evidence for these continuous layers after long conditioning periods has also been previously published (Smart, 1991). Spot analyses on the sulfide mineral surfaces after long periods of conditioning at pH 9 has shown that both pyrite and chalcopyrite surfaces are oxidized at all points measured, although the depth of oxidation in SAM depth profiles is highly variable, i.e., < 10 nm to > 300 nm (Fig. 4c).

The presence of continuous oxidized layers on chalcocite surfaces is supported by the work of Mielczarski using a combination of XPS and FTIR studies (Mielczarski and Minni, 1984; Mielczarski, 1987). The extent of surface coverage of n- and p-type chalcopyrite after exposure to oxygen or air-saturated solution has been shown to increase systematically with time (Eadington, 1968). After 30 minutes of conditioning, XPS oxygen depth profiles showed complete coverage of the chalcopyrite surface to depths averaging 6-10 nm.

The formation of a continuous oxidized surface layers is a function of oxidation environment (e.g., air, solution), time, pH, Eh and the defect properties of the sulfide mineral. The presence of the considerable number and variety of fine particles, with dimensions from < 0.1 μm to 10 μm, providing substantial coverage of larger particle surfaces (as above) helps to explain the wide variation in spot analyses from XPS and SAM surface compositions. It is apparent that even 200 μm areas of analysis can contain widely varying proportions of oxidized fine particles, flocs, and precipitated particles (Fig. 4). Nevertheless, in many cases, it is also established that sulfide surfaces can be effectively continuously covered by oxidation products, as amorphous, adsorbed layers between the particles and flocs.

**Sulfate and carbonate species**

The formation of sulfur-oxy species, particularly sulfate, as a function of time of oxidation in air or solution, has been identified in the preceding sections. Specifically, sulfate species have been observed for pyrite species in alkaline solution and in air (14 days) (Buckley and Woods, 1987). Pyrrhotite surfaces form sulfate only slowly, after more than 10 days exposure to air (Buckley and Woods, 1985a) but more rapidly in air-saturated alkaline solution (i.e., 5 minutes) (Buckley and Woods, 1985b). Grinding pyrrhotite in air increases the rate of formation of sulfate species on the surface (i.e., < 10 minutes) (Jones *et al*., 1992). Chalcopyrite exposed to air for extended periods (i.e., 10 days) shows weak sulfate peaks in the XPS S2p spectra (Buckley and Woods, 1984a; Brion, 1980). Oxidizing pentlandite surfaces in air, steam, alkaline solution or with oxidizing agents produced a surface layer which included sulfate species with the iron oxides and hydroxides (Richardson and Vaughan, 1989) although recent studies (Buckley and Woods, 1991a) of the surface composition of pentlandite under flotation-related conditions did not find that sulfate species were present unless relatively high Eh conditions in alkaline media were used. The initial oxidation of galena in air, studied by combined XPS and STM techniques, showed only the formation of carbonate, hydroxycarbonate and hydroxide species without sulfate formation (Laajalehto *et al*., 1993). Exposure of galena to air for extended periods (i.e., 4 days) resulted in sulfate formation and the binding energy of this species is more consistent with a lead hydroxy sulfate than bulk lead sulfate (Evans and Raftery, 1982; Buckley and Woods, 1984b). Lead hydroxide and lead carbonate still constitute the major part of the oxidized layer even after 10 months exposure to air. The mechanism for the dissolution of lead and sulfur from galena, via oxidation in solution near the surface, requires the formation of sulfur-oxy species which are initially soluble but may readsorb or precipitate as the oxidation/dissolution proceeds (Fornasiero *et al*., 1994).

The presence of carbonate in the oxidized surface products is not always acknowledged. It has been explicitly found on oxidized pyrrhotite surfaces (Buckley and Woods, 1985a), galena surfaces (Buckley and Woods, 1984b; Laajalehto *et al*., 1993) and in sulfide ore samples (Smart, 1991) but it is likely that it is present in surface layers of all sulfide minerals after exposure to alkaline air-saturated solution for extended periods of time.

The role of sulfate and carbonate species in directing hydrophobicity of surfaces, passivation of oxidation

reactions and insoluble precipitate formation (e.g., $CaSO_4$, $CaCO_3$) (Grano *et al*., 1995) has not been fully recognized relative to the role of hydroxides, oxyhydroxides and oxides. It is important to note that in some of these sulfide mineral systems, these species are not removed from the surface by repeated solution exchange. There is evidence, for instance, that sulfate species play a direct role in controlling pyrrhotite dissolution during ore grinding (Thomas and Smart, 1995).

Face specificity of the oxidation has been discussed in relation to the depth of the oxide layers, derived from SAM point analyses (Fig. 4c), at different places in the same chalcopyrite mineral surface (Smart, 1991). Further evidence of the distribution of the oxidation in the same pyrite:chalcopyrite system can be seen in Figure 5 where lateral distribution maps for Fe, Cu, S and O are compared before and after ion etching. On the initial surface (Fig. 5a), there is a very clear association between Fe and O with the notable exception of the much less oxidized region of dark contrast containing Point 1 of Figure 4c. It is also noted that there is a distinct line of oxidation on the chalcopyrite surface at the site of the linear defect containing Point 4 and some association with Fe along this defect. Other regions of oxidation in the O map on the chalcopyrite surface can be directly associated with $Fe(OH)_3$ flocs. Conversely, there is also a strong association between Cu and S with the notable addition of the high-sulfur region containing Point 1 on the pyrite surface. The contrast in these Auger maps depends on selection of the discrimination levels between high and low surface concentrations. Nevertheless, they clearly illustrate the much higher level of surface oxidation of the pyrite compared with the chalcopyrite surface and the exceptional nature of the small region of dark contrast on the pyrite surface.

After ion etching (Fig. 5b), interpretation of the images is more difficult but it is clear that most of the oxidation products have been removed with the exception of large floc aggregates and regions shadowed from the ion beam (i.e., close to the edges of the pyrite overlap with the chalcopyrite surface). Similarly, signals for S have been exposed in both the pyrite and chalcopyrite surfaces in all regions except those where oxidation remains. The Cu map distinguishes the regions shadowed from the ion beam because the Cu concentration on the initial surface is higher than that even on the chalcopyrite surface after ion etching. This result may indicate some preferential sputtering of Cu by the ion beam since the surface concentrations are lower than those expected for the clean chalcopyrite surface.

These and other analyses from different spots on the same particle surface of either pyrite or chalcopyrite strongly suggest that different depths of oxidation are found where fracture has exposed different facets of the mineral structure. High index faces may be expected to oxidize faster, or deeper, in the same time period, whilst analyses like that from Point 1 above suggest that some faces or regions of the surface are relatively unreactive. The ability of xanthate ions to displace oxidation products and adsorb must, at least in part, be determined by these differences in oxidation depths.

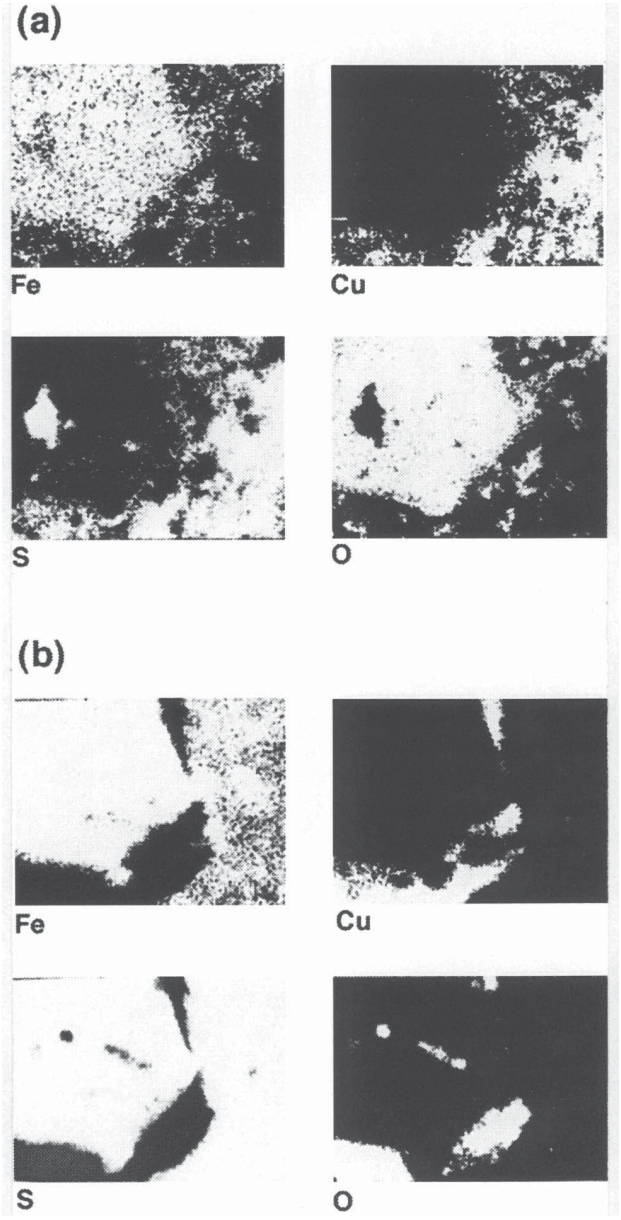


**Figure 5**. SAM elemental distribution maps from the region in Figure 4c for (**a**) Fe, Cu, S, O on the initial surface and (**b**) Fe, Cu, S, O after ~300 nm ion etch.

The development of isolated, patchwise oxidation in air and solution has been very well illustrated by STM

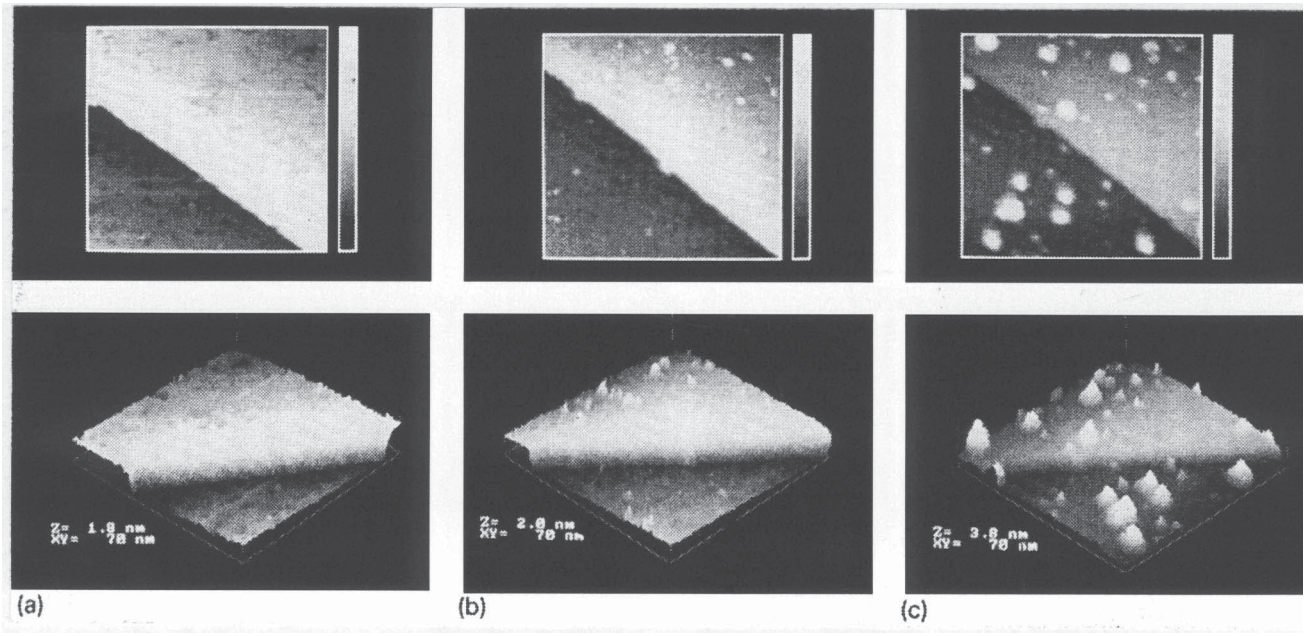


**Figure 6**. STM images from a 70 x 70 nm area of: (**a**) freshly cleaned galena surface; (**b**) the same surface after 70 minutes standing in air; (**c**) after 270 minutes in air. The upper row are grey-scale images; the lower row are 3-D (rotated) images with the vertical scales 1.8, 2.0 and 3.8 nm, respectively. Constant current mode (0.2-0.25 nA), bias ~0.35 V.

studies of galena surfaces. Eggleston and Hochella (1990, 1991, 1992) have imaged (001) surfaces of galena at atomic scale after exposure to water for 1 minute. Apparent vacancies at the sulfur sites are correlated with oxidation in their model of this process. The oxidized regions do not initiate randomly but, once oxidation has begun at a site, these regions tend to nucleate and grow without initiation of new sites. The boundaries of the oxidized regions tend to lie along the [110] directions apparently due to S atoms across this front having only one nearest neighbor oxidized sulfur, whereas an unoxidized S across a [100] boundary would have two nearest neighbor oxidized sulfurs. As with crystallization processes, [100] fronts move fast and disappear, leaving the slow moving [110] dominant.

At lower magnification, the process of galena oxidation in air has also demonstrated random sites of oxidation and growth on (001) galena surfaces with no clear preference for initiation at step edges or corners (Laajahleto *et al*., 1993). This process is illustrated in Figure 6 from that work and correlated with XPS spectra showing that the initial oxidation products are peroxide, hydroxide and carbonate species successively (see above). With time up to 270 minutes in air, the oxidation products grow from surface features with lateral dimensions < 0.6 nm through to overlapped regions > 9 nm in diameter with "holes" in the overlayer still allowing access to the underlying sulfide surface. Further studies of galena oxidation in air (Kim *et al*., 1994), comparing synthetic and natural galena samples, confirmed the growth mechanism on natural galena with the oxidation initiation sites correlated with impurity atoms in the surface layer. The much slower oxidation of synthetic galena did occur preferentially on edges, dislocations and lattice defect sites on the (001) faces of the galena crystal. The XPS spectra in this case show predominantly lead hydroxide and sulfate with a smaller contribution from carbonate in the oxidation products. In solution, STM (and AFM) imaging showed the development of sub-nanometer pits with increasing reaction time in air-purged water at pH 7 (Fig. 7) (Kim *et al*., 1995). The boundaries of the pits lie in the (100) and (010) directions in the galena surface with depths corresponding to unit cell dimensions of galena (i.e., 0.3, 0.6 nm). The process occurring in solution is congruent dissolution, confirmed by XPS spectra showing unaltered Pb4f and S2p signals.

The x-, y-dimensions of the pits and their rates of formation depend strongly on the pH and purging gas (i.e., $O_2$, air, $N_2$) used (Fig. 8). Dissolution rates, determined directly from STM images of monolayers removed, decrease with increasing pH in agreement with the reported dissolution studies on galena (Hsieh and Huang, 1989;

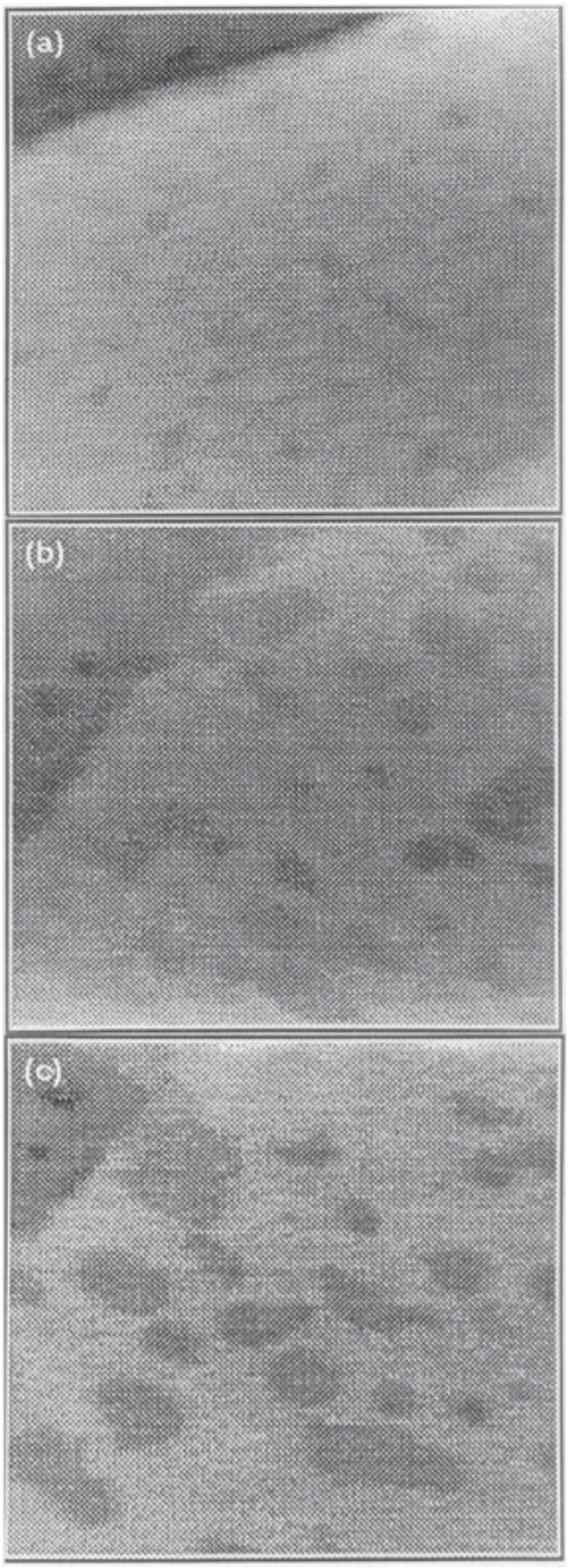


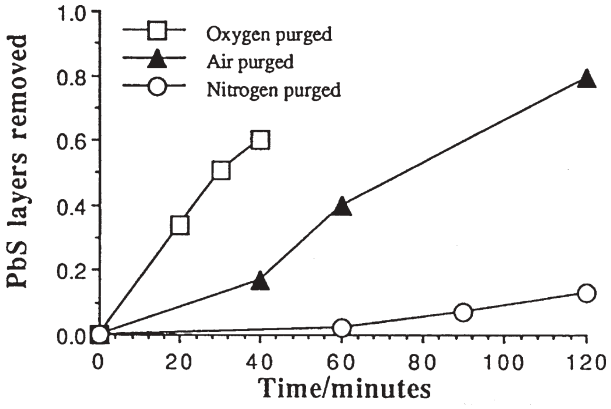


**Figure 8**. The number of equivalent lead sulphide monolayers removed from the galena surface: as a function of time in air-purged water, at different pH values (**a**) and as a function of time in water at pH 7, with different purging gases (**b**).

**Figure 7**. *(at left)* STM top-view images of galena in air purged water at pH 7 (xy scale = 500 nm): (**a**) 20 minutes, z scale = 1.7 nm; (**b**) 40 minutes, z scale = 2.1 nm; and (**c**) 60 minutes, z scale = 1.8 nm. Conditions as for Figure 3.

---

Fornasiero *et al*., 1994). For all pH values studied, the growth of the dissolution pits is significantly greater in the x- and y-directions than in the z-direction, suggesting that the edges are more active towards dissolution than the faces (Kim *et al*., 1995). At the relatively low surface area-to-volume ratios used in the STM studies, there is no evidence for the growth of surface oxidation products similar to those observed in air or to adsorption/precipitation of lead hydroxide colloids from solution. Increasing the lead ion concentration to $10^{-3}$ M in solution resulted in surface product formation with a distinct [110] directionality (Fig. 3) (Kim *et al*., 1995).

The pH dependency of galena dissolution is consistent with the mechanism proposed by Hsieh and Huang (1989) where surface protonation occurs initially as:

$$PbS + 2H^{+} \rightarrow PbSH_2^{2+} \quad (3)$$

followed by oxygen adsorption:

$$PbSH_2^{2+} + 2O_2 \rightarrow PbSH_2^{2+}\cdot(O_2)_2 \quad (4)$$

and the dissolution step:

$$PbSH_2^{2+}\cdot(O_2)_2 \rightarrow Pb^{2+} + SO_4^{2-} + 2H^{+} \quad (5)$$

It should be noted that under strongly acidic conditions or mechanical shearing action (e.g., cyclosizer),

there is XPS evidence for incongruent dissolution with the formation of a metal-deficient sulfide surface as discussed in previous sections.

## Actions of Collector Molecules

Having established the modes of oxidation in sulfide mineral conditioning, it is now appropriate to consider the effects of adsorption of selective collector molecules on the metal sulfide surfaces and the oxidation products, in their various forms, found on these surfaces.

In the context of complex sulfide ores, from previous work (Clifford *et al*., 1975; Clifford *et al*., 1975; Grano *et al*., 1990; Smart, 1991; Stowe *et al*., 1995), a number of general observations of the effects of conditioning and collector reagents in operating flotation circuits have already been made. For instance, considerable reduction in hydroxide concentration on the sulfide minerals in concentrates compared with these concentrations in conditioned feed and tails samples, is a general observation from XPS studies (Smart, 1991).

Removal of hydroxide layers by steam cleaning (Smart, 1991), dithiophosphate addition (Grano *et al*., 1995), grinding and reducing environments (Grano *et al*., 1990) and the addition of complexing agents for metal hydroxide species (Grano *et al*., 1990) have all been observed. The surface layers of concentrate samples, however, still have a relatively complex composition even when quite high grades of the concentrates are obtained. In order to understand the processes producing changes in the chemical and physical nature of the sulfide minerals during flotation, we will describe the actions of collector molecule adsorption in different modes, with case studies from literature and our recent research, namely: (**1**) adsorption to specific surface sites; (**2**) colloidal precipitation of metal-collector species from solution; (**3**) detachment of oxidized fine sulfide particles from larger particle surfaces; (**4**) detachment of colloidal metal oxide/hydroxide particles and flocs; (**5**) removal of adsorbed, oxidized surface layers; (**6**) inhibition of oxidation; (**7**) disaggregation of larger particles and; (**8**) patchwise or face-specific coverage.

In relation to these modes, the role of the collector in sulfide ore flotation has been reviewed previously (Shannon and Trahar, 1986; Richardson, 1995). Interference by metal hydroxides, in addition to collector adsorption to create hydrophobic surfaces, has been a generic theme in these reviews. Shannon and Trahar (1986) note that the function of added collector may, in some cases, be primarily to counteract the hydrophilic effects of metal hydroxides (by participating in side reactions with oxidation products) rather than to directly increase the hydrophobic character of the floating minerals. It has been shown (Buckley and Woods, 1991b) that the coverage of xanthate required on freshly abraded galena surfaces to give flotation response may constitute only a small fraction of a monolayer, a result which is in accord with plant practice where xanthate concentrations used usually correspond to < 10% of monolayer coverage of the selected sulfide mineral.

## Actions of Collectors: Case Studies

### Adsorption to specific surface sites

The selective flotation of sulfide minerals is normally carried out using thiol-based collectors including xanthates (alkyl dithiocarbonates) (X), dialkyl dithiophosphates and dithiophosphinates (DTP) and dialkyl dithiocarbamates. Early theories of collector adsorption have been refined to the currently accepted mixed potential model in which reaction between the collector and a specific surface site takes place by an anodic process with dissolved oxygen reduced at other surface sites to remove the electrons donated by the oxidation process.

$$X^- \rightarrow X_{ads} + e^- \quad (6)$$

$$MS + 2X^- \rightarrow MX_2 + S + 2e^- \quad (7)$$

$$O_2 + 4H^+ + 4e^- \rightarrow 2H_2O \quad (8)$$

where $X_{ads}$ represents an adsorbed xanthate molecule.

The mechanism has been reviewed by Richardson (1995) including the necessity for the presence of oxygen in the adsorption process. The S entity may, as previously discussed, be in the form of a metal-deficient sulfide or polysulfide species rather than elemental sulfur.

With xanthate adsorption, oxidation to dixanthogen at the surface or in solution may provide a mechanism additional to the charge transfer chemisorption of the xanthate ion, i.e.,

$$2X^- \rightarrow X_2 + 2e^- \quad (9)$$

The expectation is that any of these four species (i.e., $X_{ads}$, $MX_2$, S, $X_2$) constitute entities contributing to the hydrophobicity of the surface.

Direct observations of xanthate adsorption and the molecular form of the collector molecules have been provided by the extensive XPS, synchrotron and FTIR studies of Buckley, Mielcarzski, Suoninen and their colleagues using idealized metal and sulfide surfaces. The specific interaction of xanthate with copper atoms and ions has been widely studied in the work of Mielczarski and Suoninen on elemental copper substrates (Mielczarski *et al*., 1983; Kartio *et al*., 1994). With conventional XPS, adsorption to monolayer coverage is observed but, with

the very high surface sensitivity of synchrotron radiation, an additional S2p doublet is found attributed to different binding of the $CS_2$ group between the first chemisorbed monolayer and subsequent layers deposited over the first layer in pH 9.2 with 6 x $10^{-5}$ M ethyl xanthate for 1 minute. Further consideration of experimental factors in XPS studies of xanthate adsorption on metal and mineral surfaces (Johansson *et al*., 1986) has confirmed this interpretation and explained the dominating role of preadsorbed contaminants in alternative interpretations (Pillai *et al*., 1983). Orientation in the first monolayer also explains the relative intensities of C1s, S2p and O1s spectra with the thiol groups at the copper surface and the methyl groups furthest from the interface.

Xanthate adsorption on Cu(II) activated pyrite shows that the oxidation state of copper is changed to Cu(I) before xanthate adsorption (Smart, 1991; Szargan *et al*., 1992). Both copper xanthate and iron hydroxy xanthate species are inferred from the spectra for air-saturated neutral to alkaline (i.e., < pH 10) $10^{-4}$ M xanthate solutions. Dixanthogen is only formed and adsorbed on the pyrite surface at Eh values above 400 mV. The work has recently been reviewed (Suoninen and Laajahleto, 1993).

On copper-activated sphalerite surfaces (Prestidge *et al*., 1994) with low copper (II) additions and high affinity adsorption behavior, copper (I) ethyl xanthate is the predominant surface species. The rate and extent of ethyl xanthate adsorption are, however, decreased by extended conditioning periods apparently due to penetration of copper ions into the zinc sulfide lattice confirmed by XPS depth profiling. Time dependence of xanthate adsorption is then related to subsequent back diffusion to the solid-aqueous solution interface. At high copper additions, both dixanthogen and copper (I) ethyl xanthate are detected on the sphalerite surface but this appears to be a precipitation mechanism rather than surface reaction (see next section).

The presence of adsorbed xanthate on freshly fractured galena surfaces has been confirmed from both S2p spectra and the more surface sensitive X-ray induced Auger spectra (i.e., LMM and Pb NOO) signals. This work (Buckley and Woods, 1991b) has correlated xanthate coverage (using voltammetry) with XPS spectra and flotation recovery showing that only a fraction of the monolayer is adsorbed at maximum recovery. Sub-monolayer, perpendicularly-oriented adsorbed lead ethyl xanthate was confirmed in combined XPS, FTIR and controlled potential studies (Laajahleto *et al*., 1991). There is some contention in different literature (Leja, 1982; Page and Hazell, 1989) that pre-oxidized galena surfaces are either necessary for xanthate adsorption or facilitate the adsorption of xanthates. According to Buckley and Woods (1991b), xanthate is adsorbed immediately on freshly exposed galena surfaces following immersion in air-saturated solutions at pH 9.2. The coverage varies from 0.15 after 10 minutes to 0.37 after 1 hour in $10^{-4}$ M solution. Surface oxidation must therefore be concurrent with adsorption if this is necessary for uptake of the xanthate. The results from STM studies of surface oxidation of galena in solution, with congruent dissolution forming (100)-based pits rather than oxidation products, are also not consistent with the requirement for pre-oxidation of the surface (Kim *et al*., 1995). Precipitation of lead xanthate species may, however, result from this oxidation/dissolution reaction either *in situ* or in solution.

The influence of grinding on single and mixed mineral systems with collector adsorption has been studied by Cases' group using a combination of FTIR and XPS (Cases *et al*., 1989, 1990a,b; Kongolo *et al*., 1990). For pyrite, the results were essentially similar to those discussed above with dixanthogen and iron hydroxyxanthate as the main species. On galena, they found monocoordinate lead xanthate, non-stoichiometric and stoichiometric lead xanthate and amyl carbonate disulfide species. Dixanthogen is formed in a second adsorption stage at higher surface coverage corresponding to complete flotation and a sharp decrease in zeta potential.

The detection of collector molecules on mineral surfaces from operating flotation plants has also been confirmed by XPS (Clifford *et al*., 1975; Smart, 1991). More recently, a series of studies using TOF-SIMS by Chryssoulis and his group (Chryssoulis *et al*., 1992, 1994, 1995) and by Brinen and co-workers (Brinen and Reich, 1992; Brinen *et al*., 1993) have confirmed that this technique can distinguish fragment ions from the collectors and spatially map their distribution on single mineral grains. Sphalerite particles lost to scavenger tails have been shown (Chryssoulis *et al*., 1995) to have less amylxanthate and isobutylxanthate compared to sphalerite recovered to the zinc final concentrate. Xanthates were also detected on the surface of sphalerite particles into a copper/lead final concentrate. The face specificity of adsorption of DTP collectors will be discussed in the final section.

**Precipitation from solution**

There are now many examples of studies in the literature in which uptake of the collector molecules on the sulfide mineral surface occurs through the formation of colloidal metal-xanthate or metal-hydroxyxanthate species in solution. In some cases, it is likely that these colloidal particles form close to the surface as a result of dissolution of metal ions or reaction with the oxidation product sites on the surface. Hence, precipitation from solution may imply several different processes resulting in adsorbed precipitates.

For instance, Plescia (1993) used a combination of XRD and SEM to show that lead ethyl xanthate nucleates and crystallizes on small isolated areas of a galena surface in contact with $10^{-2}$ M ethyl xanthate solution. The kinetics

of the formation of the crystalline, mainly stoichiometric $PbX_2$, show that there is widespread nucleation in the first few minutes but the initial crystallites tend to dissolve. After 5 minutes, the crystalline form becomes stable and the kinetics of growth can be related to xanthate concentration, temperature and the oxidation state of regions on the galena surface. The presence of pre-oxidized regions or parallel oxidation/xanthate adsorption may be necessary for the formation of precipitates of lead xanthate (Page and Hazell, 1989). *In situ* STM images of a freshly cleaved galena crystal in contact with an air equilibrated $10^{-3}$ M ethyl xanthate solution are shown in Figure 9. Colloidal particles of lead ethyl xanthate (as confirmed by XPS and FTIR) form at the surface and correspond to multilayer surface coverage:

$$nPbS + 2xEX^- \rightarrow Pb_{n-x}S_n \cdot xPb(EX)_2 + 2xe^- \qquad (10)$$

*In situ* STM studies of ethyl xanthate treated pre-oxidized galena surfaces have shown the removal of oxidized lead species and the formation of colloidal lead ethyl xanthate particles (Ralston, 1994; Kim *et al*., 1995).

$$PbS \cdot yPb(OH)_2 + 2yEX^- \rightarrow PbS \cdot yPb(EX)_2 + 2yOH^- \quad (11)$$

XPS, FTIR and UV visible studies have shown that copper (I) ethyl xanthate and diethyl dixanthogen can be detected on the sphalerite surface as a result of precipitation (Prestidge *et al*., 1994). The reaction mechanism proposed is:

$$Cu^{2+} + 2EX^- \rightarrow Cu(EX)_2 \rightarrow CuEX + 1/2(EX)_2 \qquad (12)$$

It is also possible that iron hydroxy xanthate species are formed both in solution and on the surface of pyrite, contributing to its flotation behavior (Fornasiero and Ralston, 1992). A dissolution/complexation/adsorption model has been developed to explain zeta potential changes during the interaction of xanthate at concentrations from $10^{-4}$ to $10^{-3}$ M. The model suggests that, in addition to dixanthogen, these iron hydroxy xanthate complexes contribute to the flotation of pyrite as adsorbed or precipitated species.

Hence, the previously discredited reaction mechanism for sulfide mineral flotation based on the formation of insoluble metal xanthates (Taggart *et al*., 1934; Taggart, 1945; Richardson, 1995) should not be discounted. The Taggart model was criticized on the grounds that stoichiometry would require much higher collector concentration than those effective in practice (i.e., like EDTA complexation). However, the presence of precipitated, colloidal metal-collector species for lead, copper and iron with relatively low surface coverage can be demonstrated and correlated with flotation response. In some cases, e.g., galena, pyrite at Eh < 400 mV, this mechanism may be the dominant influence on flotation response. Selectivity in flotation requires that the colloidal precipitates adsorb (or form *in situ*) on sulfide particles rather than non-sulfide gangue particles. This appears likely but has not yet been directly studied.

**Detachment of oxidized fine sulfide particles**

It is generally agreed that, if sufficient hydrophilic, oxidized material is present on the mineral surfaces, this will overcome any natural or self-induced flotability as well as modifying the collector-induced flotability of the sulfide particles (Shannon and Trahar, 1986). Collector molecules are suggested to have the dual action of removing oxidized products from surfaces and providing a hydrophobic surface for bubble attachment and flotation. As demonstrated above, the forms of oxidized products on the sulfide mineral surfaces include fine oxidized sulfide particles together with colloidal metal hydroxide particles and oxidized surface layers (Smart, 1991). The surface cleaning action of xanthate has been recently reviewed by Senior and Trahar (1992) in studies of the flotation of chalcopyrite in the presence of metal hydroxides. The "cleaning" mechanism does not appear to be simple dissolution of the oxidized metals as can be achieved with other complexing agents, e.g., EDTA, because the amount of xanthate needed to restore flotability is stoichiometrically orders of magnitude below that required for the complete conversion of the metal hydroxides to dissolved metal xanthate species. This fact is also well established in plant practice where EDTA additions have been found to be effective in giving increased recovery but are prohibitively expensive.

Indications of the cleaning action in removing oxidized surface layers were noted previously (Smart, 1991). Figure 10 compares the Cu2p signals from a ground chalcopyrite sample before and after addition of $5 \times 10^{-5}$ M butyl xanthate. The initial high binding energy shoulder on the Cu2p peaks, attributed to charged hydroxide species, have been removed by the action of the xanthate.

Recent research in our group has followed the oxidation behavior of pyrite as a function of conditioning time at pH 9 under oxygen-purged conditions and the actions of xanthate adsorption.

The morphology and composition of the pyrite particle surfaces, including adsorbed oxidized particulates and overlayers, have been obtained from a SAM study whilst EDTA extraction has determined the amounts of oxidized iron species in the solution phase and on the mineral particle surfaces separately. The behavior of oxidized fine sulfide particles, with substantial hydroxide surface coverage, will clearly be similar to that of metal hydroxide precipitates and particles since their surface chemistry is closely similar. Some examples from this systematic study are selected for discussion.

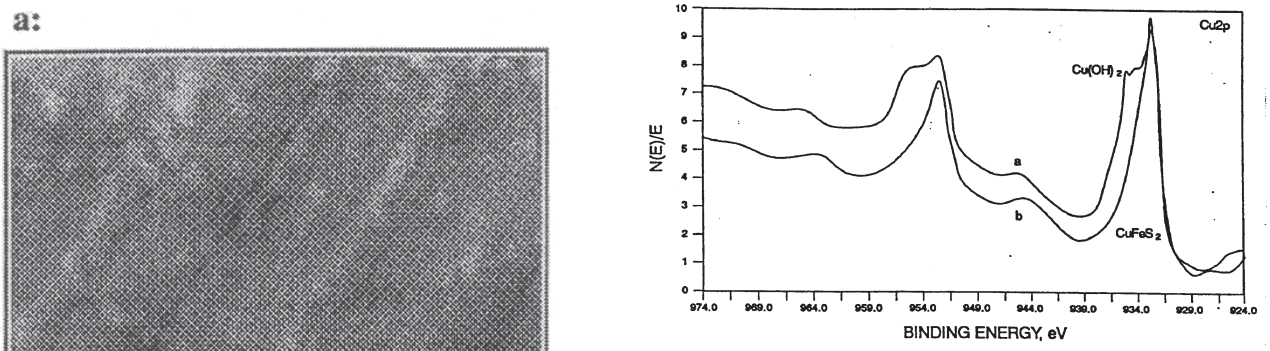


**Figure 10**. XPS Cu2p spectra from ground chalcopyrite surfaces derived from (**a**) distilled water (upper curve) and (**b**) pH 9 pulp with 5 x $10^{-5}$ M butyl xanthate addition (lower curve). Note the removal of the high binding energy copper hydroxide species after addition of xanthate collector. Some iron hydroxide remains, however, in Fe2p spectra.

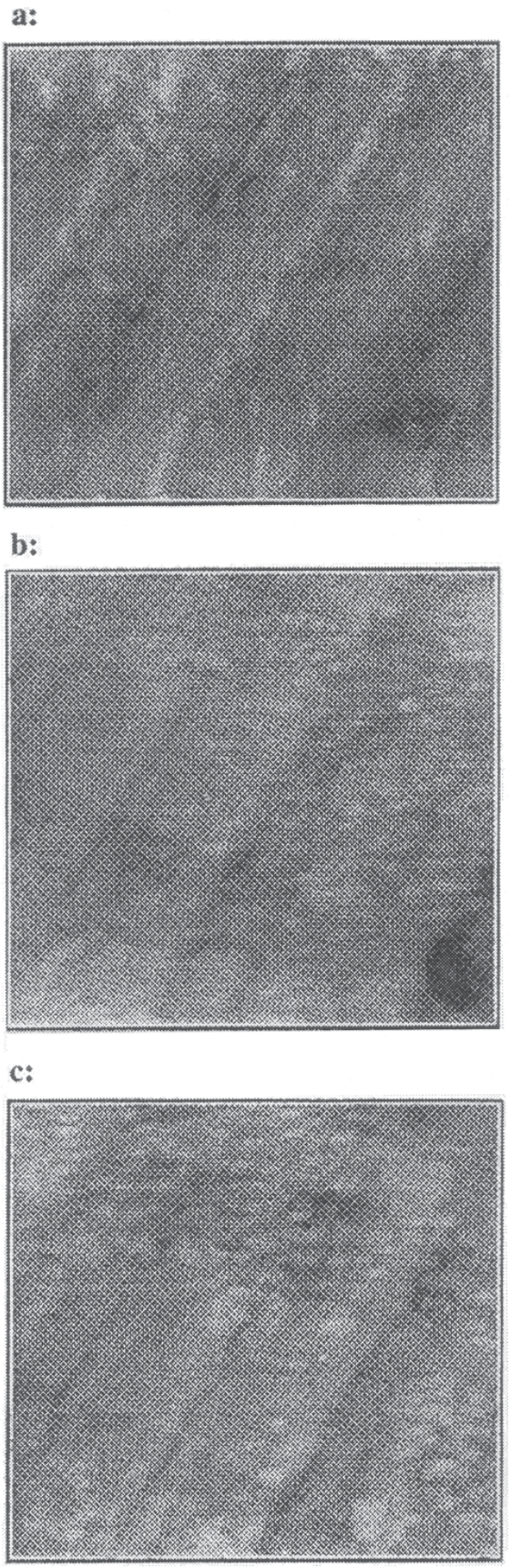


**Figure 9**. *(at left) In situ* STM images of freshly cleaved galena surface in the presence of ethyl xanthate ($10^{-4}$ M) at pH 9: (**a**) 20 minutes, (**b**) 40 minutes and (**c**) 60 minutes recorded at constant current 0.25 nA with tip bias 0.35 V. (x, y = 500 nm, z = 6.0 nm).

---

Ground natural pyrite, oxidized for 150 minutes at pH 9 under oxygen-purged conditions reveals surface features consisting of oxidized fine particles attached to larger particle surfaces together with continuous oxidized layers formed on both fine and large particle surfaces. The SAM secondary electron image and oxygen map presented in Figures 11a and 11b show clearly the surface morphology of an oxidized pyrite particle. The oxygen map shows that the colloidal precipitates at point 2 are particularly rich in oxygen as are the cleavage edges at point 3. It is also evident that oxidized products cover most of the particle surface as exemplified by point 1, an apparently featureless fracture face, free of precipitate particles.

Spot SAM analyses from points 1 and 2 are presented in Table 1 in comparison with the surface assay at the start of conditioning. Compared with the freshly ground pyrite surfaces, dramatic increases in oxygen exposure are evident both on precipitates and on fracture faces with a commensurate decrease in the sulfur signal. This together with surface iron enrichment, confirms that iron oxide/ hydroxide is present both as fine adsorbed precipitates and as a continuous overlayer on the pyrite surface.

Solution speciation calculations (Prestidge *et al.* 1995) indicate that $Fe(OH)_3$ and $Fe(OH)_4^-$ are the predominant species present under these conditions. At pH 9, $Fe(OH)_3$

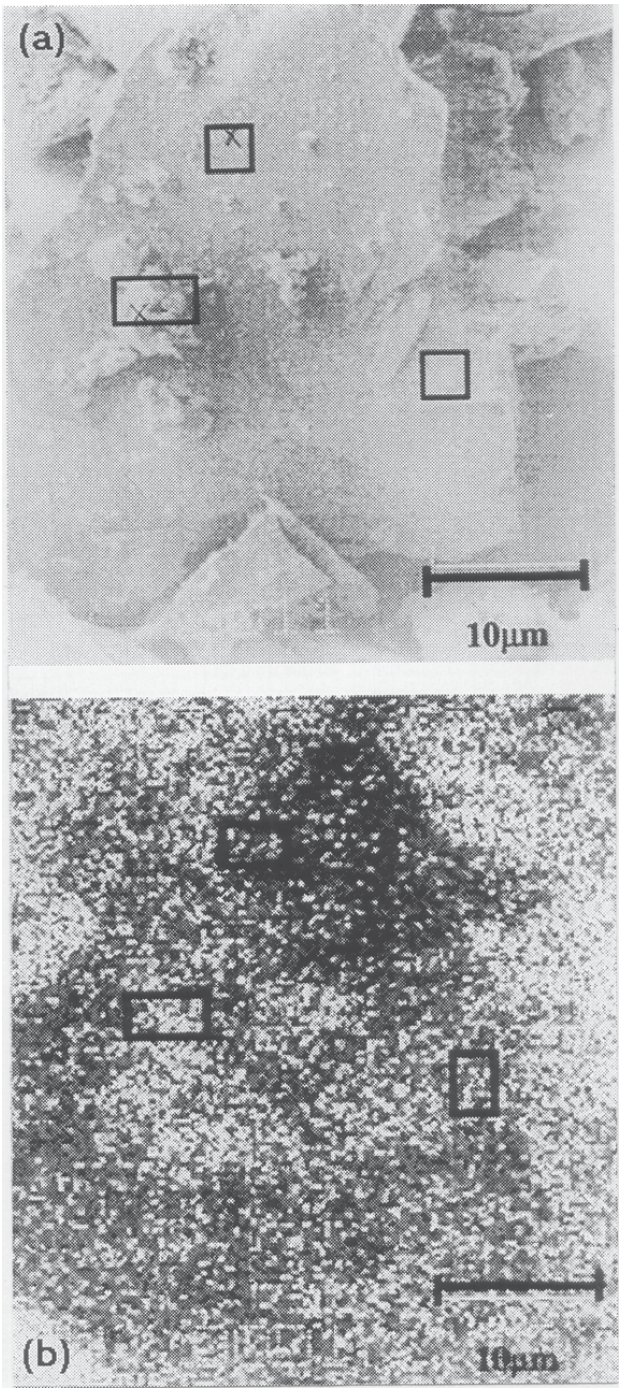


**Figure 11**. (**a**) SAM secondary electron micrograph of a pyrite particle oxidized in solution for 150 minutes at pH 9. Analysis points indicated are point 1 (top), featureless surface region; point 2 (centre), colloidal precipitate; and point 3 (right), cleavage edges. (**b**) SAM oxygen map of the same pyrite particle as in (a).

colloidal species are negatively charged (iep ~pH 6.7) as are pyrite surfaces (Fornasiero and Ralston, 1992), so it is unlikely that $Fe(OH)_3$ precipitates would adsorb by electrostatic interaction. This is supported by the results summarized in Figure 12 for iron-EDTA extraction analysis as a function of oxidation time at pH 9. It is clear that at pH 9 the majority of EDTA extractable iron is present in solution and not on the surface.

The mechanism of attachment of the oxidized fine particles and colloidal iron hydroxides must therefore rely on the *in situ* formation or hydrogen bonding between the hydroxyl groups on each surface.

Figures 13 and 14 display SAM secondary electron images of a typical pyrite particle surfaces after pH 9 oxidation for 150 minutes in the presence of $10^{-3}$ M and $10^{-5}$ M potassium ethyl xanthate (KEX), respectively. In the presence of $10^{-3}$ M KEX, there appears to be no evidence of the colloidal precipitates observed before xanthate was present. Spot analyses as indicated in Figure 13 yield the surface compositional information summarized in Table 2, which shows a complete absence of detectable oxygen together with a sulfur-enriched surface. Again considering Eh/pH stability data (Fornasiero and Ralston, 1992), the most probable iron-xanthate complex at pH 9 and high Eh is the $Fe(OH)_2EX$ species. It is also likely that, due to the highly oxidizing conditions (> 300 mV), the formation of dixanthogen ($EX_2$) may have occurred. The fact that an oxygen signal was not detectable on the particle surfaces suggests that any adsorbed oxidized iron hydroxyxanthate complexes are either in volatile form (i.e., desorbed in the ultra-high vacuum) or they have not formed. $Fe(OH)_2EX$ is not known to volatilize easily. The level of EDTA extractable iron, summarized in Figure 15, at $10^{-3}$ M KEX is extremely low from either solution or surface phase, supporting the proposition that a surface barrier or layer on the mineral surface has severely limited oxidation. The species most likely to be present on the surface is $EX_2$ which is volatile in vacuum. Pyrite surfaces exposed to such high xanthate concentrations would certainly be rendered hydrophobic, increasing their recovery to concentrates, but this concentration is well above that used in flotation. This oxidation inhibition mechanism may, however, explain different literature results and interpretation between $10^{-5}$ M and $10^{-3}$ M xanthate additions.

At a concentration of $10^{-5}$ M KEX, particle surface morphology and composition is distinctly different. Colloidal precipitates (Fig. 14, point 2) are still observed and the surface compositional results (Table 2), by virtue of significant oxygen exposure, suggest the presence of oxidized iron species. It is evident therefore that some surface oxidation still takes place on pyrite at lower xanthate concentration.

EDTA extractable iron results confirm that the effects

**Table 1**. Typical SAM spot analyses for pH 9 conditioned pyrite at start (t = 0 minutes) and end (t = 150 minutes) of conditioning.

| Analysis | Atomic concentration (%) | | | |
|---|---|---|---|---|
| | C | O | S | Fe |
| pH 9, No KEX<br>time = 0 minutes at start of conditioning | 33 | 11 | 41 | 15 |
| End of conditioning<br>time = 150 minutes | | | | |
| Spot 1: Fracture face | 24 | 28 | 19 | 28 |
| Spot 2: Colloidal precipitate | 20 | 40 | 11 | 29 |

of xanthate at $10^{-3}$ M and $10^{-5}$ M KEX concentrations are indeed very different. The level of extractable iron at $10^{-5}$ M KEX is almost an order of magnitude greater than that of the $10^{-3}$ M case and double the levels when no xanthate is present. Correlation with SAM results indicate that the passivating layer has not formed and that the dominant effect of xanthate at $10^{-5}$ M concentration is to partially clean the pyrite surface of hydroxides as they form, ensuring available iron for further oxidation and dissolution, and increased iron in solution. This mechanism is consistent with the dramatic increase in EDTA-complexable iron.

The effects of xanthate on the oxidation behavior of pyrite at pH 9 are highly dependent on xanthate concentration. At low concentrations ($10^{-5}$ M), the primary xanthate action is that of a cleaning and dispersal agent, displacing oxidized iron species from the pyrite surface, allowing further oxidation and maintaining a hydrophilic pyrite surface. At much higher xanthate concentrations ($10^{-3}$ M), the cleaned pyrite surfaces appear to be almost immediately passivated by an overlayer likely to consist of dixanthogen which, due to the high Eh conditions and high initial concentration of xanthate, may form more rapidly and segregate at particle surfaces due to its hydrophobicity. Dixanthogen is highly volatile and would not be detected in the surface by SAM under ambient ultra-high vacuum conditions.

Other examples (S. Grano and R.St.C. Smart, unpublished results) have also demonstrated dramatic reductions in surface oxygen concentration using XPS analysis. A pyrite:chalcopyrite mineral mixture ground in an iron mill gave oxygen percentages without xanthate of 41 at.% on the initial surface and 32% after ion etching to 2.5 nm depth. Addition of isobutyl xanthate at 0.1 kg/ton (i.e., ~$10^{-5}$ M) for 5 minutes to the same samples reduced the initial oxygen concentration to 21% with increased exposure of Cu (1.5x) and S (2.8x), and reduced Fe exposure (0.75x) consistent with the mechanism of surface cleaning and dispersal of iron hydroxides.

A similar action is found with the collector dicresyldithiophosphate (van der Steldt *et al*., 1993). Table 3 shows that the surface oxygen percentage is dramatically reduced by addition of 7.5 x $10^{-5}$ M at pH 4 (maximum adsorption). Removing the fine particles from the ground pyrite sample, by three successive ultrasonication/ decantation steps with solution replacement, shows that the majority of the material removed by the collector addition is in the form of fine particles rather than oxidized surface layers. Table 3 shows a level of surface oxygen concentration before fines removal similar to that after collector addition.

This surface concentration is affected by addition of the dithiophosphate collector to the deslimed pyrite sample. After collector addition, both sulfate and ferric hydroxide signals are reduced in the XPS spectra and the contamination by calcium, present on the surface before collector addition, is also removed. There has clearly been a process in which oxidized fine particles are detached from the pyrite surface by the collector addition similar to that in mechanical removal of these fine particles.

**Detachment of colloidal oxide/hydroxide particles**

Results and discussion presented in the previous section are clearly relevant to this action of collector adsorption. In addition, ethyl xanthate has been specifically shown to detach colloidal iron oxide particles (P. Bandini, C.A. Prestidge, J. Ralston and R.St.C. Smart, unpublished results) and freshly precipitated layers of ferric hydroxide (Prestidge *et al*., 1995) from galena particle surfaces. There is still some controversy on the xanthate concentrations necessary to achieve effective removal of attached particles and surface layers. In some cases, concentrations well in excess of those in flotation practice have been required to observe removal of surface oxygen (Prestidge *et al*., 1995),

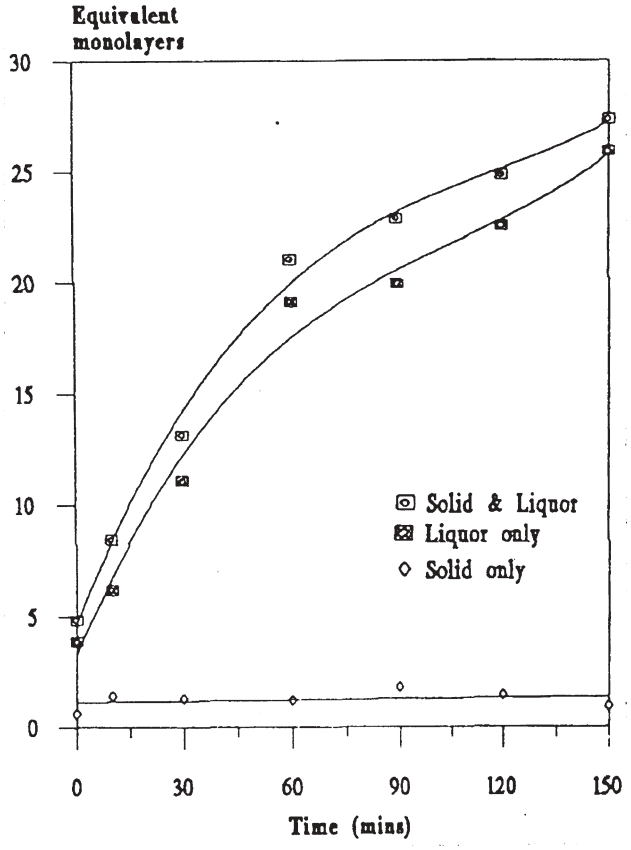


**Figure 12**. EDTA extractable iron in equivalent monolayers as a function of conditioning time at pH 9 for solid + liquor, and liquid and solid separately.

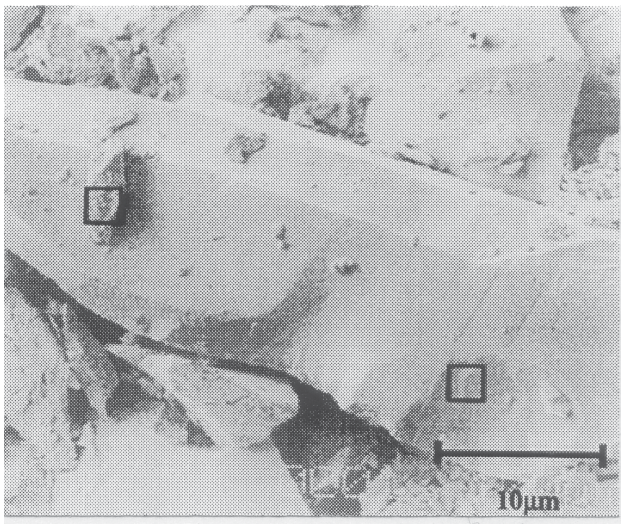


**Figure 13**. SAM secondary electron micrograph of a pyrite particle oxidized for 150 minutes at pH 9 in the presence of $10^{-3}$ M KEX. Spot 1 (right), Spot 2 (left) as marked.

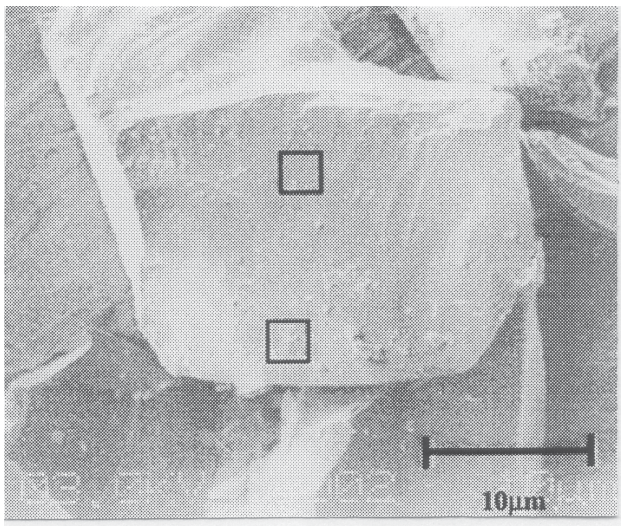


**Figure 14**. SAM secondary electron micrograph of a pyrite particle oxidized for 150 minutes at pH 9 in the presence of $10^{-5}$ M KEX. Spot 1 (upper), Spot 2 (lower) as marked.

whereas substantial reductions of oxygen concentrations have also been observed at concentrations of the order of $10^{-5}$ M xanthate (J. Grano and R.St.C. Smart, unpublished results; van der Steldt *et al*., 1993). The difference between these two concentrations may, however, lie in separation of the dispersing action, removing detached fine particles, from the complexation action dissolving oxidized surface layers. For instance, removal of $Cu(OH)_2$ precipitates, giving rise to the high binding energy component of the XPS Cu2p signals and the satellite structure for Cu(II) above 940 eV (Fig. 10), is achieved using $10^{-4}$ M ethyl xanthate solution at pH 6-10 (Szargan *et al*., 1992). In contrast, iron hydroxides are only wholly removed (i.e., quantitatively) from galena surfaces using ethyl xanthate concentrations similar to those required for EDTA complexation (i.e., > $10^{-3}$ M) (Prestidge *et al*., 1995). Separate XPS investigations (Page and Hazell, 1989; Prestidge and Ralston, 1995b) have confirmed this displacement reaction. Xanthate ions exchange with hydroxide species on the pre-oxidized galena surface to form soluble OH species (Page and Hazell, 1989). There is a significant reduction in the surface oxygen concentration according to a reaction like Equation 11.

The displacement of oxidized products by the xanthate chemisorption reaction (Eq. 11) also gives increased particle contact angle and flotability (Prestidge and Ralston, 1995b).

**Table 2**. Typical SAM spot analyses for pyrite conditioned at pH 9 in the absence and presence $10^{-3}$ M KEX.

| Auger Analysis | Atomic concentration (%) | | | |
|---|---|---|---|---|
| | C | O | S | Fe |
| pH 9, No KEX | | | | |
| time = 0 minutes | 33 | 11 | 41 | 15 |
| time = 150 minutes | | | | |
| Spot 1: Fracture face | 24 | 28 | 19 | 28 |
| Spot 2: Colloidal precipitate | 20 | 40 | 11 | 29 |
| pH 9, $10^{-3}$ M KEX | | | | |
| time = 150 minutes | | | | |
| Spot 1: Fracture face | 24 | 8 | 24 | 42 |
| Spot 2: Fine particles | 19 | 10 | 25 | 46 |
| pH 9, 10 $M^{-3}$ KEX | | | | |
| time = 150 minutes | | | | |
| Spot 1: Fracture face | 30 | < 0.1 | 38 | 31 |
| Spot 2: Fine particles | 31 | < 0.1 | 35 | 34 |

**Removal of oxidized surface layers**

Much of the discussion in the previous two sections has been concerned not only with collector displacement of oxidized fine sulfide particles and metal hydroxide colloidal precipitates but also with the actions of collectors on amorphous, oxidized surface layers. Some additional comments are, however, relevant.

Mielcarzski (1987; Mielcarzski and Minni, 1984) has proposed four stages in the mechanism of dithiophosphate interaction with chalcocite based on correlated XPS and FTIR measurements:

(**1**) In the first minute, preadsorbed hydrocarbon contaminants begin to be removed with corresponding adsorption of the collector on to the oxidized (i.e., oxide/hydroxide/carbonate) surface layer.

(**2**) Between 1-5 minutes, further removal of hydrocarbons and some oxide/hydroxide/carbonate groups continues with increasing orientation of the adsorbed molecules.

(**3**) At adsorption times of 5-15 minutes, desorption of the oxidized products is completed and a relatively well ordered, oriented layer of collector molecules is formed.

(**4**) Continuation of the adsorption process results in the formation of a layer of precipitated copper diethyldithiophosphate on top of the close packed monolayer.

Mielczarski (1986) has also observed the formation of a monolayer of iron xanthate, followed by multilayer coverage including the formation of diethyl dixanthogen and the simultaneous removal of oxidation products from marcasite surfaces.

Removal of all iron (III) species and oxidized surface layers with EDTA has been directly demonstrated by XPS (Prestidge *et al*., 1995). However, it must be pointed out that the action of xanthate in removing oxidized fine particles and surface layers is subject to the extent of prior oxidation of the mineral surface, the length of time of conditioning after xanthate addition and the subsequent length of time in the pulp solution before flotation. The presence of these oxidation products in a pyrite:chalcopyrite mixture, stored in deoxygenated solution at pH 8.5 for long periods (i.e., up to 100 days) has been demonstrated in SAM analyses with or without the addition of isobutyl xanthate ($10^{-5}$ M) to the ground product (Smart, 1991). XPS analyses using the small spot (i.e., 200 μm) XPS analyzer of the PHI 5000LS (Physical Electronics, Inc., Eden Prairie, MN) system has added some further information to the SAM analyses.

Table 4 shows the surface elemental concentrations of 6 different particles with widely varying percentages of all elements examined. The sample from which the six particles were selected in this case was that with the added isobutyl xanthate although similar results are obtained from the sample without xanthate after long storage times. The wide variation in composition between the particles is difficult to explain without the evidence from SAM (e.g., Figs. 1, 2 and 4). In general, however, there is an increase in the concentration of oxygen and a corresponding reduction in exposure of copper and sulfur signals particularly compared to the samples with xanthate addition discussed previously. The variability of the carbon percentage (i.e.,

**Table 3a**. Survey of the atomic concentrations (%) of elements for undeslimed pyrite particles conditioned at pH 4, $N_2$ purged (DCDTP = dicresyldithiophosphate).

| Element | Initial | Etch | Initial | Etch |
|---|---|---|---|---|
| | ([DCDTP] = 0 M) | | ([DCDTP] = 7.5 x $10^{-3}$ M) | |
| Carbon (C) | 28 | 7.8 | 26 | 8.3 |
| Oxygen (O) | 28 | 24 | 11 | 5.2 |
| Iron (Fe) | 10 | 27 | 21 | 39 |
| Sulfur (S) | 27 | 33 | 40 | 47 |
| Calcium (Ca) | 3.6 | 4.6 | 0.45 | < 0.05 |
| Phosphorous (P) | - | - | 0.28 | 0 |

**Table 3b**. Survey of the atomic concentrations (%) of elements for deslimed pyrite particles conditioned at pH 4, $N_2$ purged (DCDTP = dicresyldithiophosphate).

| Element | Initial | Etch | Initial | Etch |
|---|---|---|---|---|
| | ([DCDTP] = 0 M) | | ([DCDTP] = 7.5 x $10^{-3}$ M) | |
| Carbon (C) | 33 | 8.3 | 45 | 18 |
| Oxygen (O) | 13 | 2.4 | 14 | 4.0 |
| Iron (Fe) | 20 | 49 | 11 | 40 |
| Sulfur (S) | 33 | 39 | 28 | 36 |
| Phosphorous (P) | - | - | 0.47 | 0 |

15-44%) suggests that different mineral particles have considerably different surface coverages of adsorbed xanthate and, in general, it appears that more xanthate is adsorbed on surfaces with lower levels of surface oxidation as represented in the oxygen atomic concentration or, conversely, where xanthate adsorption occurs the oxygen atomic concentration is reduced through the cleaning mechanism. The analyses also suggest that, after the longer times of storage, the iron concentration is increased at the expense of the copper concentration.

The C1s spectra from both the area-average and individual particle surfaces, in addition to hydrocarbon contamination signals near 284.8 and 286.5 eV, also show a small contribution apparently due to carbonate species near 288.5 eV. The area average S2p signal (Fig. 16) shows curve fits for a sulfide doublet ($2p_{3/2}$ near 160.8 eV), a higher binding energy doublet ($2p_{3/2}$ near 162.8 eV) and a sulfate doublet ($2p_{3/2}$ near 168.6 eV). Hence, at least three different species contribute to the S atomic concentration in Table 4. The $2p_{3/2}$ sulfide peak at 160.8 eV corresponds closely to that from chalcopyrite fracture surfaces at 150 K (Buckley and Woods, 1984a). The $2p_{3/2}$ peak at 162.8 eV can be attributed to pyrite (i.e., 162.6 eV), adsorbed xanthate (i.e., 162.5 eV) (Szargan *et al*., 1992), or to a high binding energy-shifted metal deficient sulfide species from oxidation of chalcopyrite (Buckley and Woods, 1984a). The O1s spectra in all cases, i.e., area average and individual particles, were very broad (529.5-533 eV), suggesting overlap of contributions from several different species, i.e., $O^{2-}$, $OH^-$, carbonate, sulfate, etc.

The multi-species nature of other signals can also be seen in Figure 17 where the signals from Fe2p, S2p and Cu2p are compared between area average (AA) and a single particle (SP). The Fe2p spectra (Fig. 17a) clearly show that individual particles (SP) can give signals for iron sulfide species (~707 eV), whereas the overall exposure (AA) of these sulfide species, compared to the predominant ferric hydroxide species, is very low. Correspondingly, the S2p signal comparison (Fig. 17b) shows a predominant doublet with $2p_{3/2}$ near 162.8 eV (i.e., pyrite, adsorbed xanthate or metal-deficient sulfide) on the single particle with a reduced proportion of sulfate relative to the area average. The Cu2p spectra (Fig. 17c) show a higher proportion of Cu(II), seen in the shake-up satellite intensity near 944 eV, when compared with the predominantly Cu(I) species normally found on surfaces conditioned for shorter times (Smart,

**Table 4**. XPS surface concentrations (at.%) from individual particles in the set 2 sample with added isobutyl xanthate after longer storage.

| Particle | C1s | O1s | Fe2p | S2p | Cu2p3/2 |
|---|---|---|---|---|---|
| 1 | 44 | 32 | 8.7 | 12 | 3.1 |
| 2 | 27 | 48 | 50 | 19 | 2.0 |
| 3 | 36 | 40 | 6.5 | 13 | 5.0 |
| 4 | 20 | 50 | 16 | 12 | 2.6 |
| 5 | 15 | 62 | 5.3 | 16 | 1.8 |
| 6 | 20 | 58 | 8.2 | 11 | 2.9 |
| Average | 27 | 48 | 8.3 | 14 | 2.9 |

1991). The comparison between the area-average and single particle spectra also shows distinct high binding energy shoulders on both the $Cu2p_{3/2}$ and $Cu2p_{1/2}$ signals attributable to charge-shifted hydroxide, sulfate or oxide species. The intensities of these shoulders are clearly higher in the area average spectrum than the individual particle spectrum, suggesting that the more extensive xanthate adsorption on the individual particle has displaced some of this material. This result is in accord with that reported in previous work (Fig. 10); see Smart (1991) reference.

In summary, the samples after longer storage show wide variation of surface compositions of individual particles, some particles exhibiting relatively high levels of adsorbed xanthate and correspondingly lower levels of surface oxidation whilst other particles had significant increases in surface oxidation. Area-average spectra show an overall increase in surface oxidation compared with samples conditioned for shorter times and a corresponding reduction in the exposure of copper signals although all of the individual particles examined gave distinct copper surface concentration. Sulfate and carbonate species were also detected in area average and individual particle spectra. Some individual particles exposed iron as sulfides but the overall level of exposure in the area average spectra was very low, i.e., predominately as ferric hydroxide species.

The presence of the considerable number and variety of attached fine particles with dimensions from < 0.1 μm to tens of micrometers, providing substantial coverage of larger (i.e., 100-200 μm) particle surfaces as in Figure 4, helps to explain the wide variation in XPS surface compositions in Table 4. It is now apparent that 200 μm diameter areas of analysis can contain widely varying proportions of oxidized flocs, fine particles, surface layers and adsorbed species (e.g., sulfate, carbonate).

**Inhibition of oxidation**

Our SAM results, described in the section **Detachment of oxidized fine sulfide particles**, have demonstrated that, at high xanthate concentrations (i.e., $10^{-3}$ M), the formation of a surface layer, likely to consist of the oily, hydrophobic dixanthogen species, can inhibit oxidation of pyrite surfaces which would otherwise produce iron hydroxide oxidation products on the surface and in solution at lower xanthate concentrations. These results call in to question the interpretation and relevance of mechanisms derived from studies at higher collector concentrations where the collector has been added in the grinding or early in the conditioning stage.

**Disaggregation of larger particles**

The aggregation or disaggregation action of collector molecules has been difficult to quantify even in conditioned feeds to flotation. The action of aggregation caused by bubble attachment during flotation also makes it very difficult to follow in the separation between concentrate and tails. There are very few references in the literature to studies of the aggregate (rather than particle) size and composition likely to be most successfully separated in flotation.

The question of whether the addition of collectors causes aggregation or disaggregation of larger (i.e., > 5 μm particles) appears to depend heavily on the conditions under which the collector is added. In high intensity conditioning (i.e., > 850 rpm), shear flocculation can occur (Warren, 1992). In normal conditioning and flotation, xanthates have been suggested (Laskowski and Ralston, 1992) to act in a similar manner to classical dispersing agents, e.g., hexametaphosphates. Their effectiveness in dispersing the particles clearly depends on such factors as: selective adsorption; surface charge on the minerals and colloids, i.e., pH relative to iep values; ionic strength of the solution, i.e., dissolved species; and surface coverage. These factors are highly variable between different flotation pulps and in different laboratory experiments.

A direct comparison of the dispersing action of ethyl xanthate with anionic dispersants (e.g., polyphosphates)

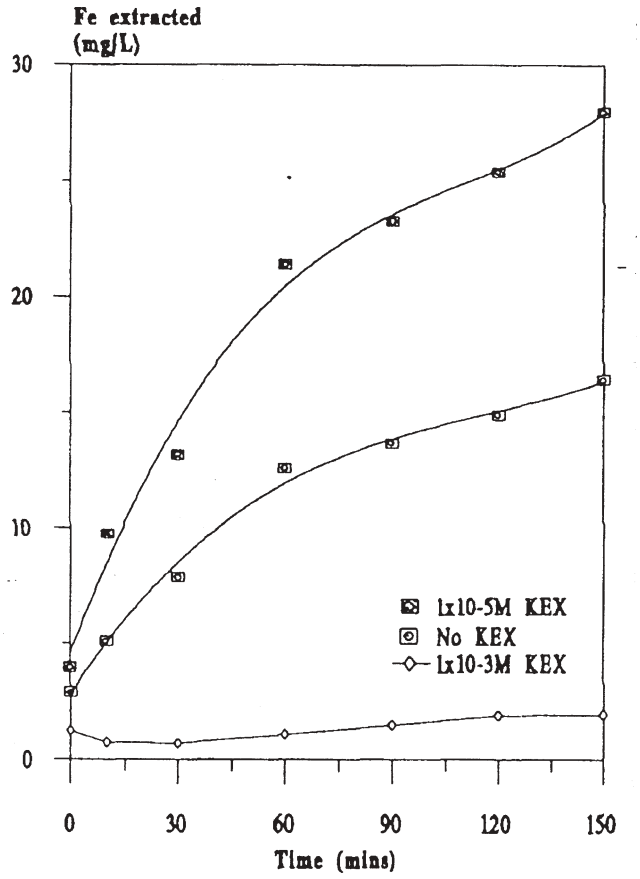


**Figure 15**. EDTA extractable iron from pyrite as a function of conditioning time at pH 9 in the presence of no KEX, $10^{-5}$ M KEX and $10^{-3}$ M KEX.

(unpublished results) has been made for iron oxide/hydroxide on quartz surfaces. Full dispersion is only achieved at xanthate concentrations greatly in excess of those generally used in flotation practice. Nevertheless, the results described above in which colloidal oxidized fine particles are detached from galena and other sulfide surfaces does suggest that the collector may have a role, albeit a minor one, in disaggregation under normal flotation conditions. This action of collectors deserves more systematic study than it has yet received.

In several industrial research projects (AMIRA, 1992, 1994, 1995) and in experience from plant practice, changes in the particle size distribution can be directly related to the addition of collector, its concentration, point of addition (e.g., during grinding, before or after cyclone classification) and length of conditioning time.

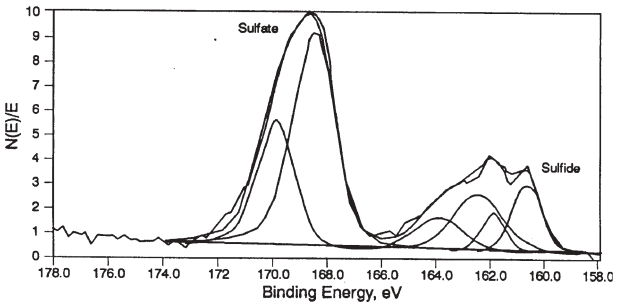


**Figure 16**. XPS area average S2p spectra three curve fitted doublets for $S2p_{1/2}$ (2:1 intensities, separation 1.2 eV) components corresponding to sulfide, adsorbed xanthate (or metal-deficient sulfide) and sulfate (see text).

**Patch-wise and face-specific collector interaction**

The observation of patch-wise attachment of colloidal lead xanthate from *in situ* studies of ethyl xanthate-treated galena surfaces (Kim *et al*., 1995) has been previously described (Fig. 9). The formation and attachment of precipitated species can clearly give rise to relatively low surface coverages in isolated regions or patches.

The early microradiographic analysis of Plaksin *et al*. (1957) first proved that the xanthate distribution on the galena surface was not uniform and that an increase in xanthate uptake did not necessarily result in increased flotation recovery. More recently, Brinen and co-workers (Brinen and Reich, 1992; Brinen *et al*., 1993) have used TOF-SIMS, in near static SIMS conditions, to detect and map the distribution of dithiophosphinate on galena crystal surfaces. Non-uniform adsorption was directly observed from 5 x $10^{-6}$ M solution conditioning for 5 minutes at pH 6-8. The concentrate from flotation (+75-150 μm fraction) was examined. The studies provided evidence to suggest that adsorption of the collector occurred in oxygen-rich areas and that there is some face-specificity on single galena particles. The uneven distribution of dithio-phosphinates is attributed to mineral surface heterogeneity arising from defects, impurities, lattice imperfections and small variations in stoichiometry but the correlation with oxygen-rich areas strongly supports the mechanism of parallel oxidation/ adsorption or adsorption on to pre-oxidized areas of the galena surfaces discussed in previous sections. TOF-SIMS has also been used by Chryssoulis and colleagues (Chryssoulis *et al*., 1995; Stowe *et al*., 1995) to image a mixture of amyldithiophosphate and amylxanthate on laboratory-treated mineral surfaces. The distribution of these reagents was again distinctly non-uniform.

To date, no direct imaging and mapping of the

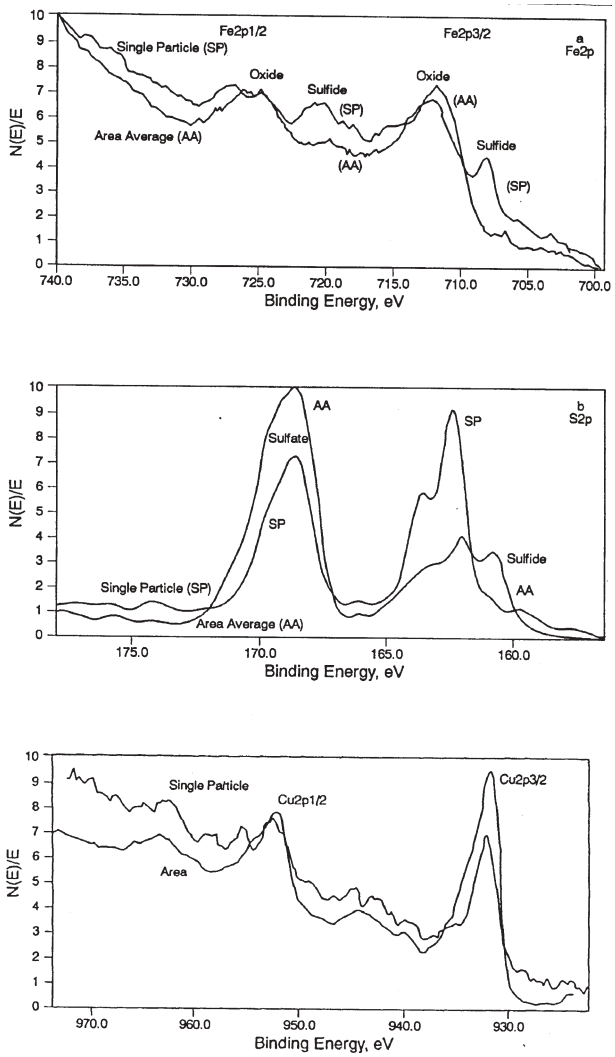


**Figure 17**. XPS spectra comparing area average (AA) and single particle (SP) surface analysis for (**a**) Fe2p, (**b**) S2p and (**c**) Cu2p regions.

distribution of collectors on sulfide surfaces other than galena have been published. It remains to be seen whether the DTP and xanthate adsorption systems on galena surfaces, in which colloidal precipitates are known to form, is a specific example of non-uniform coverage or whether this phenomenon is general. Correlation of xanthate and other collector distributions with oxidized and unoxidized regions of sulfide surfaces in, for instance, pyrite and copper-activated sphalerite flotation systems is an obvious extension of the highly sensitive TOF-SIMS technique.

## Implications for Flotation Practice

It may be thought that these examples of mechanisms of surface oxidation of sulfide minerals and the actions of collector adsorption in modifying this surface chemistry now provide a respectable body of work on which to base strategies for improved flotation practice. However, these mechanisms are much more complex, diverse and interactive than we might have envisaged even ten years ago. Our understanding of the factors directly influencing flotation in any particular set of conditions is still rudimentary. More questions are generated by each attempt to systematically analyse the effect of one particular variable. It remains true (Shannon and Trahar, 1986) that flotation "operation is usually knife-edged, control difficult and results variable."

Nevertheless, there are some examples in which the surface analytical studies, combined with flotation metallurgy and solution chemistry, have directly contributed to improvements in flotation recovery and grade.

For example naturally floatable iron sulfides have been identified and separately removed in copper flotation at Mount Isa (Grano *et al.*, 1990). This study also identified the selective removal of ferric hydroxides and carbonates by collector addition. Characterization of flotation products from a lead-zinc-copper concentrator in southeastern Missouri using XPS (Clifford *et al.*, 1975) verified the action of surface modifiers used in conditioning and correlated their surface concentrations and oxidation states with flotation response. The study noted that lead in the bulk galena-chalcopyrite scavenger concentrate was significantly more oxidized than the lead in the bulk galena-chalcopyrite rougher concentrate. The effects of fine grinding on flotation performance have been surveyed in a correlated XPS-flotation study (Frew *et al.*, 1994a) and specific application to the zinc regrind at Cominco Alaska's Red Dog mine has been reported (Frew *et al.*, 1994b). The action of an extended period of aerated conditioning before copper activation and collector conditioning in increasing sphalerite flotation at the Murchison Zinc (Western Australia) concentrator (Kristall *et al.*, 1994) was explained, using XPS, by the removal of zinc hydroxides from sphalerite surface and the concomitant appearance of a metal-deficient sphalerite surface. XPS also demonstrated an increase in the oxidation state of pyrite after aerated preconditioning. The presence of excessive surface oxidation in copper reflotation at Western Mining Corporation's Olympic Dam operation (Smart and Judd, 1994), identified by XPS analysis, led to improved operation of Lasta filters. A low flotation rate of galena in lead roughers at the Hilton Concentrator of Mt. Isa Mines was analysed (Grano *et al.*, 1993, 1995) using XPS. The presence of precipitated species and their removal by a change of conditioning reagents (i.e., lime to soda ash) and collector reagent (i.e., ethyl xanthate to

dicresyldithiophosphate, a collector stable in the presence of sulfite species over a wide pH range) has been used to address this problem.

A variety of industrial research projects, not normally reported in the literature, have used and are now using these techniques in relatively routine studies (AMIRA, 1992, 1994, 1995; Chryssoulis *et al*., 1992, 1994, 1995; Stowe *et al*., 1995).

## Remaining Research Issues

In several parts of the discussion in this review, it will be apparent that there are unresolved questions relating to both oxidation mechanisms and collector adsorption mechanisms. In some cases, argument continues concerning the nature of surface species, in other cases there are conflicting research results on nominally similar systems and, in yet other cases, alternative explanations for observed phenomena do not have direct evidence to substantiate one or other hypothesis. We will summarize some of these issues in this section.

### Oxidation mechanisms

Surface species confined to literally the top atomic layer of the sulphide surfaces have only recently been revealed by synchrotron XPS studies of sulphide surfaces before oxidation. The application of this highly surface-sensitive technique to the definition of these species in the top layer, sub-surface and bulk of the sulphide during oxidation will considerably assist our understanding of the oxidation mechanisms.

The sites of oxidative attack on the different mineral sulphide surfaces are not yet well defined. Evidence for oxidation at steps, edges and corners on pure minerals have been found but impurity sites appear to dominate oxidative attack on natural mineral surfaces. Chemical and structural information at the atomic level is still needed to define the mechanisms of oxidation in air and in different solution conditions. This is likely to come from the scanned probe microscopies (STM and AFM), particularly as their compositional capabilities are extended.

The question of the relevance of *ex situ* surface analytical results to real flotation conditions requires further correlation of these techniques with *in situ* studies from FTIR, Raman spectroscopy and the scanned probe microscopies. The body of evidence from XPS, SAM, SEM and TOF-SIMS now available provides impressive correlations with chemical changes expected in oxidation, collector adsorption and flotation processing but independent verification will continue to be required in closely correlated studies.

In collectorless flotation, the species responsible for hydrophobicity and bubble-particle attachment in flotation still generates intense discussion at meetings concerned with the surface chemistry of flotation of sulfide minerals. The contenders, metal-deficient sulfide surfaces, polysulfides and elemental sulfur, each have strong support groups. The review has discussed specific examples of conditions where one or another of these species has been reliably shown to dominate the surface layers. In many other cases, this distinction is much less obvious and highly technique-dependent. For instance, extraction of the same surfaces with ethanol or cyclohexane produces elemental sulfur with the first solvent but not with the second solvent. In cases where elemental sulfur has been extracted from the surface into the solution phase, surface analytical techniques suggest that the elemental sulfur was not present in the surface layers before extraction (i.e., metal-deficient sulphide or polysulphide species only were found). Hence, the surface species may be altered by interaction with the solvent. Studies of the species present on mineral surfaces concentrated in the flotation process, using both *ex situ* and *in situ* techniques, may help to resolve conditions under which one or another of these species is responsible for flotation.

The chemical forms and distribution of non-colloidal oxidized species on surfaces are still significantly uncertain. In some cases, high surface concentrations of sulphate cannot be associated with stoichiometric amounts of cations, relatively thick surface layers of apparently soluble species are found and they are not removed by agitation or ultrasonication, and the thickness of these layers varies from a few nanometers to hundreds of nanometers over the same particle surface. The development of these surface layers over time in different solution conditions will require study over many years.

Differences in oxidation between particles of different size have been noted in many research papers. These differences may be confined to rates of oxidation related to surface area and defect site concentrations but it is also possible that other mechanisms (e.g., surface free energy differences, impurity segregation, fracture faceting) may be directing these processes. More systematic study of particle size effects in oxidation of specific minerals is still required.

The specific question (discussed in the review) of the reason for no apparent change in the S2p XPS signals on oxidation of galena requires resolution. Under different conditions, diffusion of $Pb^{2+}$ into the metal-deficient sites, attenuation of signals by oxidized overlayers and, in solution, congruent dissolution (with precipitation of lead oxide/hydroxide), have all been suggested but evidence for each still requires validation.

### Collector adsorption and reaction mechanisms

Perhaps the most obvious issue requiring further research lies in studies of the collector species that directly

contribute to flotation. This will require comparison of concentrate with tails samples during flotation separation. The majority of research to date has focussed on the conditioned mineral before flotation separation. Very few studies comparing species between concentrate and tails have been reported.

Conflicting results from different techniques and different adsorption conditions have been reported on the association of adsorbed collector with oxidized or non-oxidized regions of sulfide mineral surfaces. This question has not yet been systematically studied, despite the variety of mechanisms postulating hydroxide displacement, metal or sulfide site attachment and colloid displacement. More direct evidence correlating *in situ* scanned probe microscopy studies with XPS, SAM and TOF-SIMS would increase our confidence in these mechanisms.

A related question concerns the role of colloidal metal-collector species. Are these formed by replacement of adsorbed OH species (or colloids) by the collector anion during adsorption or does the metal-collector species form first in solution and then displace metal hydroxide colloids? Do metal-hydroxy-collector species form on surfaces? The presence of metal-collector colloids on surfaces has been clearly established but the mechanism of their formation or attachment requires clarification.

The lateral distribution of collector species on sulfide mineral surfaces has now been shown by a variety of techniques to be non-uniform but it is not yet clear whether this non-uniformity is determined by faceting, oxidation, colloid growth and adsorption and/or defects.

There are some examples in the literature of major differences in behavior of the mineral surfaces between high ($> 10^{-3}$ M) and low (e.g., $10^{-5}$ M) collector concentrations. Differences in the structure and reactivity of the adsorbed layer and the sulfide surface are implied by these results but there are very few reports in the literature. This question is potentially of major importance because mechanisms derived at one concentration may not be applicable to another concentration (i.e., flotation conditions).

There are also conflicting reports in the literature regarding the tendency of collector molecules to cause aggregation or disaggregation of particles under different conditions of concentration, shear and pH. This aspect of flotation related to collector adsorption would benefit from systematic study but reliable observations of particle size distribution changes are difficult to achieve.

There is no shortage of interesting and useful research problems in the application of surface analytical techniques to the understanding of mechanisms in the flotation separation of minerals to occupy us into the future.

**Acknowledgements**

Much of the work reported here has involved extensive collaboration with other members of the Ian Wark Research Institute, namely Professor John Ralston, Dr. Daniel Fornasiero, Mr. Angus Netting, Dr. Pawittar Arora, Mr. Darren Simpson and Ms Angela Lange (Thiel). Collaboration with Dr. John Frew, Mr. Kevin Davey and Mr. Ross Glen at CSIRO Division of Minerals is also gratefully acknowledged. The assistance of the Australian Mineral Industries Research Association (Dr. Jim May, Mr. Bruce Fraser, Mr. Phillip Campbell and Mr. David Stribley) in providing support for more than eight years of research under industrial contracts has been of paramount importance. In particular, valuable discussions with industrial sponsors has provided much of the focus for this work, particularly: Dr. Bill Johnson (MIM); Mr. Geoff Richmond (Aberfoyle); Dr. Ian Clark, Dr. Greg Lane (Western Mining Corporation); Dr. Mike Fairweather (Cominco). The Australian Research Council has also provided funding for parallel fundamental studies in a Senior Research Fellowship (R.St.C.S.) and Research Fellowship (C.A.P.).

**References**

Ahlberg E, Forssberg KSE, Wang X (1990) The surface oxidation of pyrite in alkaline solution. J Appl Electrochem **20**: 1033-1039.

AMIRA (1992) Project P260. Interaction of iron sulfide minerals and their influence on sulfide mineral flotation. Ralston J, Smart RStC (eds.). Australian Minerals Industry Research Association. Melbourne, Australia.

AMIRA (1994) Project P336. The methods and benefits of fine grinding ores. Napier-Munn TJ (ed.). Australian Minerals Industry Research Association. Melbourne, Australia.

AMIRA (1995) Project P397. Investigation of high energy conditioning as a pretreatment for fine particle flotation. Jameson G, Ralston J (eds.). Australian Minerals Industry Research Association. Melbourne, Australia.

Arbiter N, Fujii U, Hansen B, Raja A (1975) Surface properties of hydrophobic solids. In: Advances in Interfacial Phenomena in Particulate/Solution/Gas Systems: Applications to Flotation Research. Somasundaran P, Grieves RB (eds.). American Institute of Chemical Engineering, NY. pp. 176-182.

Brinen JS, Reich F (1992) Static SIMS imaging of the adsorption of diisobutyl dithiophosphinate on galena surfaces. Surf Interface Anal **18**: 448-452.

Brinen JS, Greenhouse S, Nagaraj DR, Lee J (1993) SIMS and SIMS imaging studies of adsorbed dialkyl dithiophosphinates on PbS crystal surfaces. Int J Min Proc **38**: 93-109.

Brion D (1980) Etude par spectroscopie de photoelectrons de la degradation superficielle de $FeS_2$, ZnS et PbS a l'air et dans l'eau. (Photoelectron spectroscopic study of the surface degradation of $FeS_2$, ZnS and PbS in air and water). Appl Surf Sci **5**: 133-152.

Buckley AN (1987) The surface oxidation of cobaltite. Aust J Chem **40**: 231-9.

Buckley AN (1994) The application of X-ray photoelectron spectroscopy to flotation research. Colloids Surf A **93**: 159-172.

Buckley AN, Riley KW (1991) The self-induced flotability of sulfide minerals: Examination of recent evidence for elemental sulfur as being the hydrophobic entity. Surf Interface Anal **17**: 655-659.

Buckley AN, Woods R (1984a) An X-ray photoelectron spectroscopic study of the oxidation of chalcopyrite. Aust J Chem **37**: 2403-13.

Buckley AN, Woods R (1984b) An X-ray photoelectron spectroscopic study of the oxidation of galena. Appl Surf Sci **17**: 401-414.

Buckley AN, Woods R (1985a) X-ray photoelectron spectroscopy of oxidized pyrrhotite surfaces. I. Exposure to air. Appl Surf Sci **2/23**: 280-287.

Buckley AN, Woods R (1985b) X-ray photoelectron spectroscopy of oxidized pyrrhotite surfaces. II. Exposure to aqueous solutions. Appl Surf Sci **20**: 472-480.

Buckley AN, Woods R (1987) The surface oxidation of pyrite. Appl Surf Sci **27**: 347-452.

Buckley AN, Woods R (1991a) Surface composition of pentlandite under flotation-related conditions. Surf Interface Anal **17**: 675-680.

Buckley AN, Woods R (1991b) Adsorption of ethyl xanthate on freshly exposed galena surfaces. Colloids Surf **53**: 33-45.

Buckley AN, Woods R (1994) On the characterization of sulfur species on sulfide mineral surfaces by XPS and Raman spectroscopy. J Electroanal Chem **370**: 295-296.

Buckley AN, Hamilton IC, Woods R (1985) Investigation of the surface oxidation of sulfide minerals by linear potential sweep voltammetry and X-ray photoelectron spectroscopy. In: Flotation of Sulfide Minerals. Forssberg KSE (ed.). Elsevier, Amsterdam. pp. 41-60.

Buckley AN, Woods R, Wouterlood HJ (1989a) Surface characterization of natural sphalerites under processing conditions by X-ray photoelectron spectroscopy. In: Proc. Int. Symp. Electrochemistry in Mineral and Metal Processing II. Richardson PE, Woods R (eds.). Electrochemical Soc, Inc, Pennington, NJ. pp. 211-233.

Buckley AN, Woods R, Wouterlood HJ (1989b) An XPS investigation of the surface of natural sphalerites under flotation-related conditions. Int J Min Proc **26**: 29-49.

Buckley AN, Wouterlood HJ, Woods R (1989c) The surface composition of natural sphalerites under oxidative leaching conditions. Hydrometallurgy **22**: 39-56.

Cases JM, de Donato P, Kongolo M, Michot L (1989) An infrared investigation of amyl xanthate adsorption by pyrite after wet grinding at natural and acid pH. Colloids Surf **36**: 323-338.

Cases JM, Kongolo M, de Donato P, Michot L, Erre R (1990a) Interaction between finely ground galena and pyrite with potassium amylxanthate in relation to flotation. 1. Influence of alkaline grinding. Int J Min Proc **28**: 313-337.

Cases JM, Kongolo M, de Donato P, Michot L, Erre R (1990b) Interaction between finely ground galena and pyrite with potassium amylxanthate in relation to flotation. 2. Influence of grinding media at natural pH. Int J Min Proc **30**: 35-68.

Chryssoulis SL (1994) Mineral surface characterization by TOF-LIMS and TOF-SIMS. AMTEL Report no. 21. Univ. West. Ontario, London, Canada.

Chryssoulis SL, Stowe KG, Reich F (1992) Characterization of composition of mineral surfaces by laser-probe microanalysis. Trans Inst Min Met C **101**: c1-c6.

Chryssoulis SL, Kim J, Stowe KG (1994) LIMS study of variables affecting sphalerite flotation. In: Proc 26th Canad Min Proc Conf. Buckingham L, Robles E (eds.). Advanced Mineral Technology Laboratory, London, Ontario. Paper no. 28. pp. 1-15.

Chryssoulis S, Stowe K, Niehuis E, Cramer HG, Bendel C, Kim J (1995) Detection of collectors on mineral grains by TOF-SIMS. Trans Inst Min Met C **101**: C1-C6.

Clifford RK, Purdy KC, Miller JD (1975) Characterization of sulfide mineral surfaces in froth flotation systems using electron spectroscopy for chemical analysis. Amer Inst Chem Eng Symp Series (NY) **71**: 138-147.

Eadington P (1968) Study of the oxidation layers on surfaces of chalcopyrite by use of Auger electron spectroscopy. Trans Inst Min Metall **77**: C186-C189.

Eggleston CM, Hochella MF Jr (1990) Scanning tunneling microscopy of sulfide surfaces. Geochim Cosmochim Acta **54**: 1511-1517.

Eggleston CM, Hochella MF Jr (1991) Scanning tunneling microscopy of galena (100) surface oxidation and sorption of aqueous gold. Science **254**: 983-986.

Eggleston CM, Hochella MF Jr (1992) Tunneling spectroscopy applied to PbS(001) surfaces: Fresh surfaces, oxidation and sorption of aqueous Au. Amer Mineral **78**: 877-883.

Evans S, Raftery E (1982) Electron spectroscopic studies of galena and its oxidation by microwave-generated oxygen species and by air. J Chem Soc Faraday Trans **78**: 3545-3560.

Fornasiero D, Ralston J (1992) Iron hydroxide complexes and their influence on the interaction between

ethyl xanthate and pyrite. J Colloid Interface Sci **151**(1): 225-235.

Fornasiero D, Li F, Ralston J, Smart RStC (1994) Oxidation of galena surfaces. I. X-ray photoelectron spectroscopic and dissolution kinetics studies. J Colloid Interface Sci **164**: 333-344.

Forssberg KSE (ed.) (1986) Flotation of Sulfide Minerals. Elsevier, Amsterdam. pp.

Frew JA, Smart RStC, Manlapig EV (1994a) Effects of fine grinding on flotation performance: Generic statements. Proceedings of the Fifth Mill Operators' Conference. Aust Inst Min Metall, Melbourne, Australia. pp. 245-250.

Frew JA, Davey KJ, Glen RM, Smart RStC (1994b) Effects of fine grinding on flotation performance: Zinc regrind at Cominco Alaska's Red Dog Mine. In: Proceedings of the Fifth Mill Operators' Conference. Aust Inst Min Metall, Melbourne, Australia. pp. 287-288.

Fuerstenau MC (ed.) (1976) Flotation (A.M. Gaudin Memorial). Vols. 1 and 2. Soc Min Eng, Amer Inst Min Met Pet Eng, NY. pp. 28-29.

Fuerstenau MC, Miller JD, Kuhn MC (1985) Chemistry of Flotation. Soc Min Eng, Amer Inst Min Met Pet Eng, New York, NY. pp. 28-29.

Grano S, Ralston J, Smart RStC (1990) Influence of electrochemical environment on the flotation behavior of Mt. Isa copper and lead-zinc ore. Int J Min Proc **30**: 69-97.

Grano SR, Lauder DW, Johnson NW, Sobieraj S, Smart RStC, Ralston J (1993) Surface analysis as a tool for problem solving: A case study of the Hilton concentrator at Mt. Isa Mines Ltd. Proc Symp Polymetallic Sulfides Iberian Pyrite Belt. Portug Min Ind Assoc, Lisbon. Sect. **3-13**: 1-15.

Grano SR, Wong PL, Skinner W, Johnson NW, Ralston J (1995) Detection and control of calcium sulfate precipitation in the Hilton concentrator of Mt. Isa Mines, Ltd., Australia: Proceedings of the XIX International Mineral Processing Congress. Am Inst Miner Metall Eng Publ, San Francisco. pp. 171-179.

Greet C, Smart RStC (1996) The effect of size separation by cyclosizing and sedimentation on mineral surfaces. Miner Eng, in press.

Guy PJ, Trahar WJ (1985) The effects of oxidation and mineral interaction on sulfide flotation. In: Flotation of Sulfide Minerals. Forssberg EC (ed.). Elsevier, Amsterdam. pp. 28-46.

Heyes GW, Trahar WJ (1984) The flotation of pyrite and pyrrhotite in the absence of conventional collectors. In: Proc Int Symp Electrochemistry in Min Met Proc. Richardson PE, Srinivasan S, Woods RC (eds.). Electrochemical Soc, Inc, Pennington, NJ. pp. 219-232.

Hochella MF Jr (1995) Mineral surfaces: Their characterization and their chemical, physical and reactive natures. In: Mineral Surfaces. Vaughan DJ, Pattrick RAD (eds.). Chapman and Hall, London, UK. pp. 17-60.

Hsieh YH, Huang CP (1989) The dissolution of PbS in dilute aqueous solutions. J Colloid Interface Sci **131**: 537-549.

Johansson K-S, Juhanoja J, Laajalehto K, Suoninen E, Mielcarzski J (1986) XPS studies of xanthate adsorption on metals and sulfides. Surf Interface Anal **9**: 501-505.

Jones CF, LeCount S, Smart RStC, White T (1992) Compositional and structural alteration of pyrrhotite surfaces in solution: XPS and XRD studies. App Surf Sci **55**: 65-85.

Karthe S, Szargan R, Suoninen E (1993) Oxidation of pyrite surfaces: A photoelectron spectroscopic study. Appl Surf Sci **72**: 157-170.

Kartio I, Laajalehto K, Suoninen E (1994) Application of electron spectroscopy to characterization of mineral surfaces in flotation studies. Colloids Surf **93**: 149-158.

Kelebek S, Smith GW (1989) Collectorless flotation of galena and chalcopyrite: correlation between flotation rate and the amount of extracted sulfur. Min Metall Process **6**: 123-129.

Kim BS, Hayes RA, Prestidge CA, Ralston J, Smart RStC (1994) Scanning tunneling microscopy studies of galena: The mechanism of oxidation in air. Appl Surf Sci **78**: 385-397.

Kim BS, Hayes RA, Prestidge CA, Ralston J, Smart RStC (1995) Scanning tunneling microscopy studies of galena: The mechanisms of oxidation in aqueous solution. Langmuir, **11**: 2554-2562.

Kongolo M, Cases JM, de Donato P, Michot L, Erre R (1990) Interaction of finely ground galena and potassium amylxanthate in relation to flotation. 3. Influence of acid and neutral grinding. Int J Min Proc **30**: 195-215.

Kristall Z, Grano SR, Reynolds K, Smart RStC, Ralston J (1994) An investigation of sphalerite flotation in the Murchison Zinc concentrator. Proceedings of the Fifth Mill Operators' Conference. Aust Inst Min Metall, Melbourne, Australia. pp. 171-180.

Laajalehto K, Nowak P, Pomianowski A, Suoninen E (1991) Xanthate adsorption at lead sulfide/aqueous interfaces: Comparison of XPS, infrared and electrochemical results. Colloids Surf **57**: 319-333.

Laajalehto K, Smart RStC, Ralston J, Suoninen E (1993) STM and XPS investigation of reaction of galena in air. Appl Surf Sci **64**: 29-39.

Laskowski JS, Ralston J (eds.) (1992) Colloid Chemistry in Mineral Processing. Developments in Mineral Processing Series. Vol. 12. Fuerstenau DW (ed.). Elsevier, Amsterdam.

Leja J (1982) Surface Chemistry of Froth Flotation Plenum, NY.

Luttrell GH, Yoon RH (1984) Surface studies of the collectorless flotation of chalcopyrite. Colloids Surf **4**: 271-281.

McCarron JJ, Walker GW, Buckley AN (1990) An X-ray photoelectron spectroscopic investigation of chalcopyrite and pyrite surfaces after conditioning in sodium sulfide solutions. Int J Min Proc **30**: 1-16.

Mielcarzski J (1986) *In situ* ATR-IR spectroscopic study of xanthate adsorption on marcasite. Colloids Surf **17**: 251-271.

Mielcarzski J (1987) XPS study of ethyl xanthate adsorption on oxidized surface of cuprous sulfide. J Colloid Interface Sci **120**: 201-209.

Mielczarski J, Minni E (1984) Adsorption of diethyldithiophosphate on cuprous sulfide. Surf Interface Anal **6**(5): 222-234.

Mielczarski J, Werfel F, Suoninen E (1983) XPS studies of interaction of xanthate with copper surfaces. App Surf Sci **17**: 160-174.

Mycroft JR, Bancroft GM, McIntyre NS, Lorimer JW, Hill IR (1990) Detection of sulfur and polysulfide on electrochemically oxidized pyrite surfaces by XPS and Raman spectroscopy. J Electroanal Chem **292**: 139-152.

Mycroft JR, Nesbitt HW, Pratt AR (1995) X-ray photoelectron and Auger electron spectroscopy of air-oxidized pyrrhotite: Distribution of oxidized species with depth. Geochim Cosmochim Acta **59**: 721-733.

O'Connor J, Sexton BA, Smart RStC (eds.) (1992) Surface Analysis Methods in Materials Science. Springer-Verlag, Berlin, Germany.

Page PW, Hazell LB (1989) X-Ray photoelectron spectroscopy (XPS) studies of potassium amyl xanthate (KAX) adsorption on precipitated PbS related to galena flotation. Int J Min Proc **25**: 87-100.

Pillai KC, Young VY, Bockris JOM (1983) XPS studies of xanthate adsorption on galena surfaces. Appl Surf Sci **16**: 322-334.

Plaksin IN, Zaitseva SP, Starchik LP, Turnikova VI, Khazinskiya, GN, Shaefeyev RS (1957) An investigation of the interaction of minerals with flotation reagents by the application of microradiography. Zavodskaya Lab **23**: 313-316.

Plescia P (1993) Study of galena/potassium ethyl xanthate system by X-ray diffractometry and scanning electron microscopy. App Surf Sci **72**: 249-257.

Pratt AR, Muir IJ, Nesbitt HW (1994) X-Ray photoelectron and Auger electron spectroscopic studies of pyrrhotite and mechanism of air oxidation. Geochim Cosmochim Acta **58**(2): 827-841.

Prestidge CA, Ralston J (1995a) Contact angle studies of galena particles. J Colloid Interface Sci **172**: 302-310.

Prestidge CA, Ralston J (1995b) Contact angle studies of ethyl xanthate coated galena particles. J Colloid Interface Sci, in press.

Prestidge CA, Thiel AG, Ralston J, Smart RStC (1994) The interaction of ethyl xanthate with copper (II)-activated zinc sulfide: Kinetic effects. Colloids Surf A. **85**: 51-68.

Prestidge CA, Skinner W, Ralston J, Smart RStC (1995) The interaction of iron (III) species with galena surfaces. Colloids Surf A **105**: 325-339.

Ralston J (1994) The chemistry of galena flotation: Principles and practice. Min Eng **7**: 715-735.

Richardson PE (1995) Surface chemistry of sulfide flotation. In: Mineral Surfaces. Vaughan DJ, Pattrick RAD (eds.). Chapman and Hall, pp. 261-302.

Richardson S, Vaughan DJ (1989) Surface alteration of pentlandite and spectroscopic evidence for secondary violarite formation. Min Mag **53**: 213-22.

Senior GD, Trahar WJ (1992) The influence of metal hydroxide and collector on the flotation of chalcopyrite. Int J Min Proc **33**: 321-341.

Shannon LK, Trahar WJ (1986) The role of collector in sulfide ore flotation. In: Advances in Minerals Processing. Somasundaran P (ed.). Soc Mining Engineers, Inc, Littleton, Colorado. pp. 408-425.

Smart RStC (1991) Surface layers in base metal sulfide flotation. Min Eng **4**: 891-909.

Smart RStC, Judd B (1994) Improved Lasta filter and copper reflotation performance through surface analysis surveys at WMC's Olympic Dam Operation. In: Proceeding of the Fifth Mill Operators' Conference. Aust Inst Min Metall, Melbourne, Australia. pp. 1-4.

Somasundaran P (ed.) (1986) Advances in Minerals Processing. Soc Mining Engineers, Inc, Littleton, Colorado.

Stowe KG, Chryssoulis SL, Kim JY (1995) Mapping of composition of mineral surfaces by TOF-SIMS. Min Eng **8**: 421-430.

Suoninen E, Laajalehto K (1993) Structure of thiol collector layers on sulfide surfaces. Proc XVIII Int Min Proc Congr (Sydney, Aust). Vol. 3. Aust Inst Min Met, Melbourne, Australia. pp. 625-629.

Szargan R, Karthe S, Suoninen E (1992) XPS studies of xanthate adsorption on pyrite. Appl Surf Sci **55**: 227-232.

Taggart AF (1945) Flotation. In: Handbook of Mineral Dressing. Taggart AF (ed.). John Wiley and Sons, Inc., New York. Section 12. pp. P01-P130.

Taggart AF, del Guidici GRM, Ziehl DA (1934) The case for chemical theory of flotation. Trans AIME **112**: 348-381.

Thomas J, Smart RStC (1995) The dissolution of pyrrhotite under acidic conditions. In: Proc 10th Nat Conv. Royal Aust Chem Inst, Melbourne, Australia. pp. P130-P161.

van der Steldt K, Skinner W, Grano S (1993) A study

of the interaction of di-cresyl, dithiophosphate with galena and pyrite using micro flotation, z potential measurements and X-ray photoelectron spectroscopy. Ian Wark Research Institute Report.

Walker GW, Richardson PE, Buckley AN (1989) Workshop on the flotation-related surface chemistry of sulfide minerals. Int J Min Proc **25**: 153-158.

Wang X, Forssberg KSE, Bolin NJ (1989) Thermodynamic calculations on iron-containing sulphide mineral flotation systems. I. The stability of iron-xanthates. Int J Min Proc **27**: 1-19.

Warren LJ (1992) Shear flocculation. In: Colloid Chemistry in Mineral Processing. Laskowski J, Ralston J (eds.). Elsevier, Amsterdam. pp. 309-330.

Zachwieja JB, McCarron JJ, Walker GW, Buckley AN (1989) Correlation between the surface composition and collectorless flotation of chalcopyrite. J Colloid Interface Sci **132**(2): 462-468.

**Discussion with Reviewers**

**A.N. Buckley**: It is suggested that the reason a S2p component from a lead-deficient sulfide species is not observed for slightly oxidized galena is that such a species remains localized directly underneath the isolated Pb/O patches. Do the authors believe that such an explanation is consistent with the high mobility of Pb atoms in the galena lattice?

**Authors**: In the oxidation of galena in solution, we have shown (Kim *et al*., 1995) that congruent dissolution of Pb and S species occurs accompanied by hydrolysis and precipitation of $Pb(OH)_2$. In this case, the appearance of unaltered S2p spectra with shifted Pb4f components due to oxidized species is consistent with this mechanism. However, oxidation in air does not allow dissolution or loss of oxidized sulfur species (e.g., sulfate). It is recognized that Buckley and Woods (1984b) have shown that air oxidation of galena also produces shifted components in the Pb4f spectrum, attributed to oxidized lead species, with no change in the S2p species. This result was explained by the formation of Pb/O oxidation products removing lead atoms from the surface, the metal-deficient sulfide layer being replenished by diffusion of $Pb^{2+}$ from the bulk of the galena crystal. Diffusion of lead in galena is much faster than diffusion of iron, zinc or copper in other metal sulfides, making this explanation plausible. The argument against the hypothesis is that, under other conditions of reaction of the galena surface, such as air-saturated acetic acid solution, additional broad S2p doublets are observed at higher binding energy and these doublets shift to higher values as oxidation proceeds (Buckley and Woods, 1984b). If Pb diffusion is able to compensate for the metal-deficient sulfide generated in the first case, why is this not also true for the second case? The answer may well lie in the proportion of the surface that becomes metal-deficient by reaction. Where the proportion of the surface covered by oxidized lead products is relatively small (i.e., < 10%), either of the two explanations (i.e., lead diffusion or signal attenuation) may be true. A more remote possibility involves oxidation of $S^{2-}$ to sulfur (lost to vacuum) with reduction of oxygen to hydroxide. At this time, the authors believe that more evidence is required before an explanation can be offered with confidence.

**A.N. Buckley**: Given the proposition that in alkaline solution oxidation proceeds on galena surfaces without the formation of sulfur-rich zones, and given that oxidizing conditions are necessary for the collectorless flotation of this mineral, on what basis is the collectorless flotability of galena in alkaline solution explained?

**Authors**: Limited collectorless flotation of galena, generally to < 40% total recovery, can occur after preconditioning in alkaline solution. The collectorless flotation of sulfide minerals implies hydrophobicity of ~10% (or more) coverage of the surface layers. This can be achieved by surface reactions producing metal-deficient sulfide, polysulfides or elemental sulfur. However, there are also a number of sulfide minerals that exhibit natural flotability without preconditioning (e.g., by oxidation, dissolution), e.g., realgar, stibnite and orpiment. These minerals do not require specific Eh for flotation, nor is there any variation of flotation with Eh. A relatively non-polar surface is exposed after fracture so that the nature of the chemical bonding and crystal structure at the surface is responsible for the hydrophobicity (Arbiter *et al*., 1975). Galena does not appear to belong to this category of minerals. Also, unlike chalcopyrite in oxidizing conditions where a sulfur-rich surface layer is formed by removal of iron atoms from the surface layers, galena does not show evidence of the high binding energy-shifted S2p doublet or metal deficiency. The most likely explanation comes from the work of Prestidge and Ralston (1995a) in which it has been shown that high shear conditions in solution remove oxidized products from the surface layers, exposing hydrophobic sulfur-rich patches in the surface. The combination of shear and dilution may also enhance incongruent dissolution (Eq. 2), adding to the sulfur-rich nature of the surface. We believe that these contact angle and XPS studies add some support to our contention that the metal-deficient, sulfur-rich regions lie beneath the oxidized products giving strongly attenuated XPS signals. However, this hypothesis is by no means proven.

**A.N. Buckley**: It is claimed that there is now strong evidence that the surface phase described as a metal-deficient sulfide

is actually a polysulfide species. What is the evidence for the sulfur-rich environment formed under conditions (especially Eh and pH) of relevance to flotation being a polysulfide?

**Authors**: This question is still much discussed in the literature (Buckley and Riley, 1991; Buckley and Woods, 1994). As this review points out, the primary reaction resulting in these species is the oxidation and removal of the metal cation from the surface layers, resulting in the metal deficiency. The question of the correct description of this layer is then highly dependent on the conditions of the reaction and the subsequent restructuring in the surface layer. There is a clear example of restructuring to form a new metal-deficient surface phase, provided by X-ray diffraction evidence (Jones *et al*., 1992), where pyrrhotite transforms to a defective $Fe_2S_3$ surface product after acid reaction. This product has linear chains of $S_n$ atoms with a S-S distance similar to elemental sulfur but the S2p binding energy is still 0.2-0.6 eV less than elemental sulfur. Hence, this surface is a "metal-deficient sulphide," has a "polysulfide" chain structure and a distinct, new lattice rearrangement. There are other examples where Raman spectra corresponding closely to specific polysulfide species have been correlated with XPS S2p high binding energy doublets attributed to metal-deficient sulfide species (Mycroft *et al*., 1990). These observations were, however, made at relatively high oxidizing potentials, i.e., above 0.6 V/SCE (voltages referred to the standard calomel electrode). There are many more cases in the XPS literature where metal-deficient, sulfur-rich surface layers are observed with no parallel evidence for restructuring or molecular structure corresponding to polysulfides. At the same time, the XPS spectra do not represent elemental sulfur. It appears to us that the chemistry of increased hydrophobicity is associated with the change in S-S bonding resulting from the metal deficiency. The examples where XPS spectra have been correlated with diffraction or molecular spectroscopy tend to suggest that there is a transition from the original sulfide surface through to elemental sulfur as the extent of S-S bonding increases. In this transition, there will be specific polysulfide species $S_n^{2-}$ with different n chain links. It is highly probable that not all of these species have been characterized in molecular spectroscopy and that they are not detected until present in quite high concentrations in the surface. Nevertheless, our view is that they all constitute polysulfide species resulting directly from the metal deficiency. Under conditions of pH and Eh relevant to flotation, the increased hydrophobicity is still likely to be associated with increased S-S bonding in the metal-deficient sulfide surface. At this point in the argument, the distinction between a "metal-deficient sulfide" and a "polysulfide species" appears to become semantic. The focus must be on the chemistry of the hydrophobic entities.

**A.N. Buckley**: Reference is made to reports of uptake of colloidal metal-xanthate or metal-hydroxy xanthate species by sulfide mineral surfaces, however, these reports are usually associated with the use of high concentrations of collector. Why is this collector uptake mechanism considered to be of relevance under practical flotation conditions?

**Authors**: We do not suggest that these high concentrations of collector are relevant to practical flotation conditions. Instead, the point made in the review is that a large proportion of the literature purporting to describe mechanisms of collector adsorption and reaction relate to studies at these high (e.g., $10^{-3}$ M) concentrations. We have tried to point out that quite different mechanisms, e.g., inhibition of oxidation, formation of dixanthogen, inhibition of diffusion through hydrophobic multilayers, may occur.

However, not all of the work identifying colloidal metal-xanthate species has used high xanthate concentration. It is relevant to note that the $K_{sp}$ values of metal xanthate and metal hydroxy xanthate species, where available, strongly suggest that colloidal precipitates will be formed at xanthate concentrations of the order of $10^{-5}$ M. For example, $Pb(EX)_2$ ($K_{sp} = 2.1 \times 10^{-17}$) will form at these concentrations with lead ion concentrations of $2 \times 10^{-7}$ M, CuEX ($K_{sp} = 5.2 \times 10^{-20}$) at copper (I) concentrations as low as $10^{-15}$ M (Fuerstenau *et al*., 1985). In fact, Cases *et al*. (1990a) have observed colloidal lead xanthate at these concentrations. Iron (III) xanthates (e.g., $Fe(EX)_3$, $K_{sp} = 10^{-24}$) will form with iron concentrations of $10^{-15}$ M. The $K_{sp}$ values of iron hydroxy xanthates are more contentious but, using the values derived by Wang *et al*. (1989), we would also expect colloidal precipitation of $Fe(OH)(EX)_2$ and $Fe(OH)_2EX$ at pH 9 for iron (III) concentrations of $10^{-15}$ M and $10^{-20}$ M, respectively.

Hence, there are two separable cases. At high collector concentrations, different mechanisms of adsorption and reaction may be operating but, at concentrations similar to those used in practical flotation conditions, the presence of the colloidal species must be considered. More detailed study at the lower concentrations is obviously still required.

**A.N. Buckley**: Why do the authors believe that if the approximate correlation between oxygen-rich areas and collector-rich areas observed on galena in a non-static SIMS study is confirmed by TOF-SIMS measurements, this finding will provide strong support for either the parallel oxidation/adsorption mechanism or the adsorption on to pre-oxidized sites mechanism for collector interaction with the mineral.

**Authors**: In the mechanism proposed in Equation 11, the

xanthate ions exchange for hydroxide ions of lead hydroxy species either formed *in situ* or by colloidal adsorption from solution. If this process is incomplete, as we would expect with limited concentration of collector and an excess of oxidation products, we would expect to find the collector-rich areas associated with the oxygen-rich areas. The surfaces were conditioned with collector for approximately 5 minutes. The results from XPS analysis of closely similar systems show that the adsorption of collector reduces the oxygen surface concentration (as hydroxide) but does not remove it all. There are remaining uncertainties in this correlation. There are conflicting reports of association between oxygen-rich areas and collector-rich areas (Brinen *et al*., 1993) and oxygen-rich, collector-poor correlation (Stowe *et al*., 1995) using TOF-SIMS studies of similar collectors on galena surfaces. This mechanism is not yet proven and requires further studies of correlations in this and other mineral-collector systems.

**Reviewer II**: Many XPS studies emphasize the use of peak fitting algorithms in interpreting their spectra in which, in many cases, individual peaks are not resolved. This usually involves fitting peaks for particular chemical species of binding energies determined in studies where that species occurs in significantly different chemical environments. With what degree of confidence are you able to ascertain the individual chemical species contributing to an overall XPS spectrum such as in your Figure 16?

**Authors**: We would certainly agree that the degree of confidence in the binding energies of the fitted peaks and their attribution to individual chemical species is not high. The basis facts we have relied on in these attributions are the following:

(**1**) the binding energy of the $S2p_{3/2}$ peak of the first (lowest binding energy) doublet should correspond to the binding energy of the lowest sulfide doublet (i.e., chalcopyrite near 161.1 eV). The curved fitted value of 160.8 eV indicates the extent of error in the procedure;

(**2**) there is one or more component in the S2p spectra at higher binding energy required to fit the peak envelope. We have fitted this with a doublet ($2p_{3/2}$ near 162.8 eV) but it is clearly possible that several, or even a continuum, of components make up this high binding energy intensity. For instance, there must be components due to pyrite sulfide near 162.4 eV but there is additional intensity at higher binding energy than this value. We have not attempted to assign these binding energies to specific species but simply to claim that the curve fit can be attributed to a combination of pyrite sulfide, adsorbed xanthate and metal-deficient sulfide;

(**3**) the curve fit to the highest binding energy doublet is closely consistent with sulfate species adsorbed on sulfide mineral surfaces. These binding energy values are relatively well established in the literature and do not vary significantly between different sulfides. The curve fit is, in this case, reasonably reliable.

**Reviewer II**: You mention that STM work, among other techniques, is needed on sphalerite. Considering the relatively higher band gap characteristic of sphalerite, how would you approach this problem?

**Authors**: The presence of relatively minor concentrations of impurities (e.g., 10-20 ppm Fe) in natural sphalerite makes this mineral much more conductive than pure ZnS. For instance, SEM images of most natural sphalerites can be obtained without conductive coatings (e.g., C, Au). Adsorption (and incorporation) of Cu(I) on sphalerite surfaces renders the surface layers conductive as observed in the removal of charge shifting in XPS spectra. A band gap reduction (i.e., ~3.7 eV to ~0.5 eV) is well established in this case. STM images at the atomic scale are still difficult to obtain from natural sphalerites and, of course, the presence of the impurities complicates the interpretation of the surface reactions but it is possible to work with these surfaces at lower magnification (e.g., 100 x 100 nm). Copper-activated sphalerite surfaces can be imaged relatively straightforwardly in STM and this system is of direct interest to flotation separation of this mineral.

**Reviewer II**: I agree with you that surface studies have contributed significant advances in the field of sulfide oxidation. I also agree that studies meant to elucidate the mechanism underlying a macroscopic process using observations made in ultra-high vacuum (UHV) conditions must be reconciled with the observations of the phenomena operating in air or solution. What are some problems which are encountered in making this connection when it comes to sulfide oxidation?

**Authors**: The two major sets of techniques available for *in situ* reconciliation with the *ex situ* surface analytical techniques are the molecular spectroscopies (FTIR, Raman) and the scanned probe microscopies (AFM, STM). The molecular spectroscopies suffer from lack of sensitivity using low concentrations of reagents unless high surface area mineral samples are used (i.e., $>10\ m^2g^{-1}$). This means, in practice, working with only the finest fraction of particles involved in flotation separation or using much higher concentrations of reagents than are normally used in flotation practice. ATR methodologies have now been improved considerably to reduce these limitations but it still remains difficult to obtain IR or Raman spectra from the low surface coverages observable in XPS and TOF-SIMS.

The scanned probe microscopies are providing most important information on the structure and lateral distribution of adsorption and reaction down to the atomic

level but information on the chemistry of individual sites, reacted regions or adsorbed species is still very limited. The development of scanning tunneling spectroscopy and the electrochemical probe microscopies needs to be considerably advanced before a more complete correlation can be attempted. In the meantime, we are able to learn a good deal in correlated studies of XPS with STM or AFM (Laajalehto *et al*., 1993). The increasing spatial resolution of XPS analysis and imaging promises to considerably assist this interpretation as it becomes possible to analyse reacted regions at the micron and sub-micron scale.